NASA TECHNICAL MEMORANDUM

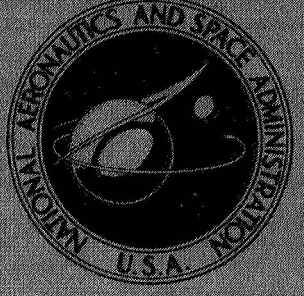

NASA TM X-2916

NASA TM X-2916

TRANSIENT RESPONSE OF SHELLS OF REVOLUTION BY DIRECT INTEGRATION AND MODAL SUPERPOSITION METHODS

by Wendell B. Stephens and Howard M. Adelman

Langley Research Center
Hampton, Va. 23665

NATIONAL AERONAUTICS AND SPACE ADMINISTRATION • WASHINGTON, D. C. • MAY 1974

1. Report No. NASA TM X-2916	2. Government Accession No.	3. Recipient's Catalog No.
4. Title and Subtitle TRANSIENT RESPONSE OF SHELLS OF REVOLUTION BY DIRECT INTEGRATION AND MODAL SUPERPOSITION METHODS		5. Report Date May 1974 6. Performing Organization Code
7. Author(s) Wendell B. Stephens and Howard M. Adelman		8. Performing Organization Report No. L-9216 10. Work Unit No. 502-32-01-02
9. Performing Organization Name and Address NASA Langley Research Center Hampton, Va. 23665		11. Contract or Grant No. 13. Type of Report and Period Covered Technical Memorandum
12. Sponsoring Agency Name and Address National Aeronautics and Space Administration Washington, D.C. 20546		14. Sponsoring Agency Code
15. Supplementary Notes		

16. Abstract

This report describes the results of an analytical effort to obtain and evaluate transient response data for a cylindrical and a conical shell by use of two different approaches: direct integration and modal superposition. The purpose of the investigation was twofold: to provide reliable data for use in the checkout of general-purpose codes and to gain some insight into the relative advantages of each technique.

The principal conclusions drawn from the present study are that for the types of problems investigated herein, the inclusion of nonlinear terms is more important than the inclusion of secondary linear effects (transverse shear deformation and rotary inertia) although there are thin-shell structures where these secondary effects are important. The advantages of the direct integration approach are that geometric nonlinear and secondary effects are easy to include and high-frequency response may be calculated. In comparison to the modal superposition technique the computer storage requirements are smaller. The advantages of the modal superposition approach are that the solution is independent of the previous time history and that once the modal data are obtained, the response for repeated cases may be efficiently computed. Also, any admissible set of initial conditions can be applied.

17. Key Words (Suggested by Author(s))	18. Distribution Statement
Direct integration Modal superposition Transient response Shells of revolution	Unclassified – Unlimited STAR Category 32

19. Security Classif. (of this report)	20. Security Classif. (of this page)	21. No. of Pages	22. Price*
Unclassified	Unclassified	53	$3.75

*For sale by the National Technical Information Service, Springfield, Virginia 22151

TRANSIENT RESPONSE OF SHELLS OF REVOLUTION BY DIRECT INTEGRATION AND MODAL SUPERPOSITION METHODS

By Wendell B. Stephens and Howard M. Adelman
Langley Research Center

SUMMARY

This report describes the results of an analytical effort to obtain and evaluate transient response data for a cylindrical and a conical shell by use of two different approaches: direct integration and modal superposition. The purpose of the investigation was twofold: to provide reliable data for use in the checkout of general-purpose codes and to gain some insight into the relative advantages of each technique.

Results are obtained for the cylindrical shell which is freely supported at both edges and for the conical shell which is freely supported at the small diameter and free at the large diameter. Both shells are subjected to an initial velocity excitation. Both the direct integration analysis and the modal superposition analysis included such secondary effects as rotary inertia and transverse shear deformation. As a result, the importance of these effects as well as the ease of their inclusion in the calculations were evaluated. In addition, the numerical integration analysis included nonlinear effects due to large displacements. Consequently, the importance of these effects was evaluated also.

The principal conclusions drawn from the present study are that for the types of problems investigated herein, the inclusion of nonlinear terms is more important than the inclusion of secondary effects although there are thin-shell structures where these secondary effects will be important. The advantages of the direct integration approach are that geometric nonlinear and secondary effects are easy to include and high-frequency response may be calculated. In comparison to the modal superposition technique the computer storage requirements are smaller. The advantages of the modal superposition approach are that the solution is independent of the previous time history and that once the modal data are obtained, the response for repeated cases may be efficiently computed. Also, any admissible set of initial conditions can be applied.

INTRODUCTION

Dynamic response behavior can be an important design consideration for thin shells of revolution which are often used as structural members in aerospace vehicles and civil

structures. As a result, there have been attempts in recent years to provide analytical procedures for accurately calculating dynamic response of general shells of revolution. The two methods that have shown the most promise for a wide variety of shell geometries are direct integration of the equations of motion by using finite differences (refs. 1 to 5) and modal superposition based on a finite-element calculation of the modal characteristics of the shell (refs. 6 to 8). Each approach is most advantageous for a certain subclass of the general problem.

Recently, the trend in analytical methods development has been toward large general-purpose computer programs (refs. 9 and 10). One important task in the development of such programs is comparing those results with the results of special-purpose codes in order to generate confidence in the minds of potential users. Thus, the purpose of the present paper is to provide some reliable results for transient response of shells of revolution for use in checking more general-purpose computer programs.

As a part of the present work, it was desirable to carry out some extensions to previous work and to develop some new procedures. These extensions are presented in three appendixes. Appendix A contains modifications to the direct integration procedure of reference 1 to include the effects of rotary inertia and transverse shear deformation. Appendix B describes the modal superposition algorithm. Appendix C describes the finite-element derivation for modal characteristics of cylindrical shells with rotary inertia and transverse shear effects included. A fourth appendix, appendix D, lists in tabular form all numerical results shown in the figures. This is provided so that meaningful checks with other analyses can be made.

SYMBOLS

$[A_k]$ matrix which relates coefficients of assumed displacements to displacements and rotations at ends of element

$a_{0,k}, a_{1,k}, a_{2,k}, a_{3,k}$ coefficients in assumed displacement function for u

$b_{0,k}, b_{1,k}, b_{2,k}, b_{3,k}$ coefficients in assumed displacement function for w

C membrane stiffness, $\frac{Eh}{1 - \nu^2}$

$[C_k]$ matrix defined in equation (C21)

$c_{0,k}, c_{1,k}, c_{2,k}, c_{3,k}$ coefficients in assumed displacement functions for β

D flexural stiffness, $\frac{Eh^3}{12(1 - \nu^2)}$

E elastic modulus

e_1, e_2 meridional and circumferential strains, respectively

$[F]$ matrix defined in equation (C12)

G shear rigidity, $\frac{E}{2(1 + \nu)}$

h shell thickness; H in computer tables

$i = \sqrt{-1}$

$\bar{K}$ total number of elements

$[K_n]$ stiffness matrix for nth harmonic

k^2 shear correction factor (0.87 for a thin shell)

L meridional length

$[M_k]$ element mass matrix

$[M_n]$ mass matrix for the nth harmonic

M_x meridional moment resultant; M-X in computer tables; MX in computer plots

$N_x, N_{x\theta}$ membrane force resultants

n positive integer; N in computer tables

Q_x transverse shear stress resultant

q_n normal coordinate of the system

$[R]$ matrix defined in equation (C7)

r radial distance; R in computer plots and tables

$[S_k]$ element stiffness matrix

s meridional coordinate; S in computer plots and tables

s_k distance from first edge of cylinder to center of kth element

T kinetic energy

t time; T in computer plots

U,V,W meridional, circumferential, and normal displacement components at any point in shell, respectively

u,v,w meridional, circumferential, and normal displacement components of point on middle surface, respectively

V strain energy (appendix C)

v_o initial velocity

$[X]$ matrix defined in equation (C17)

x meridional coordinate in a finite element

$[Y]$ matrix defined in equation (C25)

$\{y\}$ vector containing all unknown displacements and their spatial derivatives

$[Z_k]$ matrix defined in equation (C27)

z coordinate measured normal to middle surface of cylinder

$\alpha = \frac{h^2}{12}$

β rotation of a point on middle surface of cylinder

$\{\gamma\}$ vector defined in equation (C16)

γ_{13} transverse shear strain

ϵ_k length of kth element

$[\Lambda_n]$ diagonal matrix of eigenvalues for nth harmonic (appendix B)

λ_n eigenvalue of nth harmonic (appendix B)

ν Poisson's ratio

ρ mass density

$\sigma_1, \sigma_2, \sigma_{13}$ stress in the meridional, circumferential, and transverse directions, respectively

$[\Phi_n]$ matrix of eigenvectors for nth harmonic (appendix B)

$\{\phi_n\}$ eigenvector for nth harmonic (appendix B)

ψ cone angle (fig. 1(b))

ω angular frequency, rad/sec

A prime indicates a derivative with respect to the meridional coordinate s.

A dot indicates a derivative with respect to time t.

ANALYTICAL METHODS

Direct Integration

The results in this paper illustrating the direct integration method are obtained from the shell programs contained in references 1 and 3. The program in reference 1 is based on Sanders' shell theory for small displacements with moderate rotations (ref. 11). The governing equations of motion are reduced to six partial differential equations with first-order spatial derivatives and second-order time derivatives and are applicable to shells loaded axisymmetrically. The time derivatives are represented numerically by Houbolt's backward-difference expression as outlined in references 1 and 4 and the spatial derivatives are represented by central differences. The equations are linearized using a Newton-Raphson technique and solved using Gaussian elimination. Modifications to the equations contained in reference 1, for the inclusion of rotary inertia and transverse shear effects, are presented in appendix A.

Sanders' shell theory for small rotations is also used in reference 3 which deals with the asymmetric behavior of shells. The equations are written as four governing partial differential equations with second-order derivatives in both space and time. The Houbolt backward-difference scheme and central differences are again used to represent the time and space derivatives, respectively, and Gaussian elimination is used to solve the equations. Since backward differences are used to represent time derivatives, the method is dependent on the previous time history of the shell. In general, this method allows one to take moderately large time steps without detrimentally affecting the quality of convergence. For structures in which high frequencies dominate the response, very small time increments must be taken. The convergence criterion used in this report was to use a time increment such that decreasing the time increment size by a factor of 2 would not affect the results more than 1 percent after 10 time steps.

Modal Superposition

The method used for the modal superposition calculations is described in appendix B. Basically the approach is to take the stiffness and mass matrices and modal characteristics supplied by a previously executed program and compute generalized stiffness and mass matrices. These are then used to form a set of uncoupled equations which are solved in closed form for a given set of initial conditions. All supplied modes are used to preclude any arbitrary omission of modes which could have significant contributions.

The modal characteristics are supplied either by the program of references 7 and 8 or by a program based on the method described in appendix C. A critical feature of this approach is to obtain the modal data accurately. A discussion of this feature is contained in appendix C.

ILLUSTRATIVE EXAMPLES

The two shell configurations shown in figures 1 and 2 were considered. In these problems a satisfactory uniform grid spacing has been utilized unless otherwise indicated.

Cylindrical Shell

The first configuration is a cylindrical shell with freely supported boundary conditions and with a uniform initial velocity. This shell is similar to the one with cutouts used in reference 5. Since the structure has a plane of symmetry perpendicular to the shell axis and since the initial velocity is uniform, only half the structure needs to be analyzed. The boundary conditions at the initial edge ($s = 0$) are

$$N_x = 0$$

$$W = 0$$

$$M_x = 0$$

and at the plane of symmetry (s = L/2) are

$$U = 0$$

$$Q_x = 0$$

$$\beta = 0$$

The initial conditions were taken to be

$$U(s,0) = 0$$

$$V(s,0) = 0$$

$$W(s,0) = 0$$

$$\beta(s,0) = 0$$

and

$$\dot{U}(s,0) = 0$$

$$\dot{V}(s,0) = 0$$

$$\dot{W}(s,0) = 2.54 \text{ cm/sec} \quad (1.0 \text{ in./sec})$$

$$\dot{\beta}(s,0) = 0$$

where the displacements are all functions of space and time and a dot represents a derivative with respect to time. The material properties were taken to be

$$E = 6464 \text{ N/m}^2 \quad \left(0.9375 \text{ lb/in}^2\right)$$

$$\rho = 10.7 \text{ Gg/m}^3 \quad \left(1.0 \text{ lb-sec}^2/\text{in}^4\right)$$

$$\nu = 0.25$$

The dimensions of the cylinders are characterized by the length-radius ratio L/r and the thickness-radius ratio h/r. Calculations are carried out for a range of L/r from 0.3 to 2.4 and a range of h/r from 0.0125 to 0.10.

The finite-element grid used in the modal superposition method is shown in figure 3(a). For the direct integration method the spacial-difference increments used were $\Delta s = L/96$ and the nondimensional time-difference increment was taken to be 0.10 sec. The loading along the shell meridian midsurface is an inertial loading corresponding to the initial conditions on velocity.

Conical Shell

The second configuration was a cone similar to the Viking aeroshell (ref. 12). The finite-element grid of figure 3(b) is applied consistent with the geometry of figure 1(b). Here the dimensions are

$r_A = 80.0$ cm (31.5 in.)

$r_B = 164.0$ cm (64.6 in.)

$L = 89.46$ cm (35.22 in.)

$\psi = \pi/9$ (20^o)

$h = 0.101$ cm (0.04 in.)

and the material properties are

$E = 73.08\ GN/m^2$ $\left(1.06 \times 10^7\ psi\right)$

$\nu = 0.315$

$\rho = 2713\ kg/m^3$ $\left(2.54 \times 10^{-4}\ lb\text{-}sec^2/in^4\right)$

The boundary conditions are freely supported at the inner edge ($s = 0$) and free at outer edge. Therefore, at $s = 0$:

$N_x = 0$

$W = 0$

$V = 0$

$M_x = 0$

and at $s = L$:

$$N_x = 0$$

$$Q_x = 0$$

$$N_{x\theta} = 0$$

$$M_x = 0$$

The initial conditions were

$$U(s,0) = 0$$

$$V(s,0) = 0$$

$$W(s,0) = 0$$

$$\beta(s,0) = 0$$

and

$$\dot{U}(s,0) = 0$$

$$\dot{V}(s,0) = 0$$

$$\dot{W}(s,0) = -v_o \frac{(L - s)}{L} \qquad \left(v_o = 2.54 \text{ cm/sec} \quad (1.0 \text{ in./sec})\right)$$

$$\dot{\beta}(s,0) = 0$$

The finite-difference grid sizes were $L/100$ in the spacial direction and 10^{-6} sec in time increments. The nonhomogeneous, initial condition is a linearly varying normal velocity along the shell meridian with peak amplitude of v_o at $s = 0$. This provides the only loading on the structure.

RESULTS AND DISCUSSION

These results are presented for future comparisons with large general-purpose shell codes. Brief parametric studies are presented as well as a tabular listing in appendix D of all the numerical results.

Cylindrical Shell

Results for the cylindrical shell with loading corresponding to an initial velocity normal to the shell middle surface are shown in figure 4. Both the direct integration and modal superposition approaches are compared with an "exact" solution similar to that described in appendix C of reference 13. Here, the exact solution is again a modal superposition technique where all the modes were obtained as sine and cosine waves. The series summation in the solution was truncated after 100 modes. The curves in figure 4 represent the normal displacement W/r along the shell meridian at 1.2 seconds (after 12 steps in time for the direct integration scheme have been taken). The agreement is quite good except for the peak displacement region around $s/L = 0.10$ for the modal superposition approach; even then the discrepancy is only about 5 percent and this is attributed to the fact that only 10 elements were used to model the shell. The accuracy of the modal superposition approach is obviously dependent on obtaining a large number of reliable eigenvalues and eigenvectors. As the number of elements is increased, computer storage and time increase proportionally. Once the modal data are obtained, however, the modal superposition approach can be applied to any point independent of time history; in fact, repeated solutions at various points in time can be obtained quite efficiently. Since the modal data are dependent only upon the shell geometry and boundary conditions, the modal superposition approach allows an additional degree of flexibility in efficiently studying a variety of initial conditions.

Figures 5 to 8 show the effect of transverse shear deformation and rotary inertia (secondary effects) on transient response of the cylindrical shell for three values of L/r. The direct integration scheme is used to produce these results. In these figures the ratio h/r is held to a value of 0.05. In these plots the linear solution and the linear solution with the secondary effects included are compared. Figure 5 is a plot of normal displacement W/r as a function of the meridional distance at a time of 1.2 sec (12 steps in time). For this curve the secondary effects affect the solution only slightly; however, the moment resultant M_x, which has a more prominent boundary region as shown in figure 6, indicates that these terms have a more pronounced effect.

Figures 7 and 8 show that these effects also grow as the shell is shortened while the other geometrical data remain constant. Since in these figures there is no pronounced boundary-region behavior, this deviation from the linear solution is attributed primarily to the transverse-shear-deformation terms.

Figures 9 to 11 indicate the importance of being able to include nonlinear terms in the solution as well as the effect of varying the ratio h/r where the ratio L/r remains at 2.4. In these cases the direct integration scheme must be used since modal superposition is restricted to linear problems. Figure 9 is a comparison of the normal

displacement W/r along the meridian for the linear, nonlinear, and secondary effects solutions. The curves are shown at 2.4 sec (24 increments in time) for the cylinder. The secondary effects are of little importance as also shown in figure 5, but the nonlinear terms greatly affect the character of the response shape. Figures 10 and 11 show that for thinner shells these terms remain just as large and tend to damp out the response in the region around the shell edge at $s = 0$.

Figure 12 shows the results for the linear asymmetric response for the second harmonic ($n = 2$) when L/r is 2.4 and h/r is 0.05. In this figure the normal displacement is plotted as a function of meridional distance s/L at a time of 2.4 sec (24 increments in time for the direct integration scheme) for both approaches. Here the agreement of the methods is better than that in figure 4. In this case 20 elements along the meridian were taken. This better modeling improves the quality of the results; however, to obtain this accuracy all the modal data must be stored and as such may make this procedure impracticable in large-scale applications.

In figure 13 both maximum normal displacement and center displacement are plotted as a function of time for the structure when L/r is 2.4 and h/r is 0.10. The solutions give a profile of time history for linear, nonlinear, and secondary effects for axisymmetric analyses.

Conical Shell

The conical shell shown in figure 1(b) is analyzed for a load corresponding to a linearly decreasing initial normal velocity along the shell meridian. The results in figure 14 are for the normal displacement corresponding to $n = 2$ at a time of 20×10^{-6} sec (or after 20 time increments in the direct integration scheme). Satisfactory agreement is obtained by using a fine finite-element grid ($\epsilon/L = 0.025$) in the region near the smaller boundary of the shell and coarser grids with larger elements throughout the remaining portion of the shell (see fig. 3(b)). The direct integration approach gives an almost linear decay of the displacement to zero at the outer edge ($s/L = 1.0$). The small oscillatory character of the modal solution is attributed to the coarsest grid size ($\epsilon/L = 0.100$) used near the larger boundary of the shell.

The two approaches each offer unique capability. The modal approach yields numerical accuracy at any point in time. Also, the modal data are obtained independent of the initial conditions. Thus, the modal superposition results may be obtained at any time point and for any admissible set of initial conditions.

The distinctive features of the direct integration approach are that high-frequency response may be analyzed and that both secondary and nonlinear effects can be easily included.

CONCLUDING REMARKS

Both direct integration and modal superposition schemes for transient response analysis of shells of revolution have been discussed. The analysis reported in NASA TN D-6158 has been extended to include the secondary effects of rotary inertia and transverse shear deformation terms. In addition, the analytical scheme for modal superposition and a finite-element analysis for obtaining the axisymmetric mode shapes and frequencies of cylindrical shells with secondary effects included have been presented.

A brief parametric study of nonlinear and secondary effects has been shown and tabular data of the results have been made available. In general, the inclusion of nonlinear terms is of much more importance than the inclusion of secondary effects although there are thin-shell structures where these secondary effects will be important. The advantages of the direct integration approach are that geometric nonlinear and secondary effects are easy to include and high-frequency response may be calculated. In comparison to the modal superposition technique the computer storage requirements are less. The advantages of the modal superposition approach are that the solution is independent of the previous time history and that once the modal data are obtained, the response for repeated cases may be efficiently computed. Also, any admissible set of initial conditions can be used with the modal superposition method. The actual preference of one method over the other is dependent, therefore, on the problem requirements.

Langley Research Center,
National Aeronautics and Space Administration,
Hampton, Va., January 28, 1974.

APPENDIX A

MODIFICATIONS OF ANALYSIS OF NASA TN D-6158 TO INCLUDE ROTARY INERTIA AND TRANSVERSE SHEAR DEFORMATION

To include rotary inertia and shear, equations (4) and (5) of reference 1 should be replaced by

$$m'_{11} + \frac{\cos \phi}{r}(m_{11} - m_{22}) - \frac{q}{\lambda^2} + \frac{h^3}{12}\ddot{\beta} = 0 \tag{A1}$$

$$\frac{2(1 + \nu_{12})}{k^2 E_{10} h} q = w' - \phi' u - \beta \tag{A2}$$

where q is the transverse shear resultant and $\ddot{\beta}$ the rotary inertia. These changes require that equations (A6) and (A9) in reference 1 be changed to include, respectively,

$$h_{52} = -\frac{2(1 + \nu_{12})}{E_{10} h k^2} \tag{A3}$$

$$M_{26} = \frac{-h^2}{12} \tag{A4}$$

The notation of equations (A1) to (A4) is the same as that used in reference 1.

APPENDIX B

MODAL SUPERPOSITION PROCEDURE

This appendix describes the procedure based on reference 6 for obtaining the transient response of shell structures using modal superposition for problems with non-homogeneous initial conditions. In this analysis for any harmonic number n, the $m \times m$ stiffness matrix $\left[K_n\right]$, the $m \times m$ mass matrix $\left[M_n\right]$, the eigenvector matrix $\left[\Phi_n\right]$, and the eigenvalues λ_n^i where $i = 1, 2, \ldots, m$ are provided by an analysis such as that in reference 8 or that described in appendix C. The equations of motion from reference 6 may be written as

$$\left[M_n\right]\left\{\ddot{y}_n\right\} + \left[K_n\right]\left\{y_n\right\} = 0 \tag{B1}$$

where the dots indicate differentiation with respect to time. The initial conditions are

$$\left.\begin{aligned} \left\{y_n\right\} &= \left\{y_0\right\} \\ \left\{\dot{y}_n\right\} &= \left\{\dot{y}_0\right\} \end{aligned}\right\} \tag{B2}$$

Transforming to the modal coordinates $\left\{q_n\right\}$ gives

$$\left\{y_n\right\} = \left[\Phi_n\right]\left\{q_n\right\} \tag{B3}$$

where the ith column of $\left[\Phi_n\right]$, denoted as $\left\{\phi_n^i\right\}$, satisfies the equation

$$\left[K_n\right]\left\{\phi_n^i\right\} = \lambda_n^i\left[M_n\right]\left\{\phi_n^i\right\} \tag{B4}$$

with λ_n^i being the eigenvalue corresponding to the eigenvector $\left\{\phi_n^i\right\}$. The eigenvectors are normalized so that the generalized mass for each mode is unity

$$\left[\Phi_n\right]^T\left[M_n\right]\left[\Phi_n\right] = \left[I\right] \tag{B5}$$

Using equation (B5) with equation (B4) gives the additional result that

$$\left[\Phi_n\right]^T\left[K_n\right]\left[\Phi_n\right] = \left[\Lambda_n\right] \tag{B6}$$

where $\left[\Lambda_n\right]$ is a diagonal matrix of the eigenvalues. Using equations (B3), (B5), and (B6) in equation (B1) gives a set of equations for the elements of $\left\{q_n\right\}$

$$\left\{\ddot{q}_n\right\} + \left[\Lambda_n\right]\left\{q_n\right\} = 0 \tag{B7}$$

The initial conditions (eqs. (B2)) expressed in terms of $\left\{q_n\right\}$ are

$$\left.\begin{aligned} \left\{q_n\right\}_0 &= \left[\Phi_n\right]^T\left[M_n\right]\left\{y_0\right\} \\ \left\{\dot{q}_n\right\}_0 &= \left[\Phi_n\right]^T\left[M_n\right]\left\{\dot{y}_0\right\} \end{aligned}\right\} \tag{B8}$$

The solution of equation (B7) subject to the conditions of equations (B8) is easily obtained. The ith element of $\left\{q_n\right\}$ denoted as q_n^i is given by

$$q_n^i = a_n^i \sin\sqrt{\lambda_n^i}\, t + b_n^i \cos\sqrt{\lambda_n^i}\, t \tag{B9}$$

where $i = 1, 2, \ldots, m$.

$$a_n^i = \begin{cases} \dfrac{1}{\sqrt{\lambda_n^i}}\left\{\phi_n^i\right\}^T\left[M_n\right]\left\{\dot{y}_0\right\} & \left(\lambda_n \neq 0\right) \qquad \text{(B10)} \\ 0 & \left(\lambda_n = 0\right) \qquad \text{(B11)} \end{cases}$$

$$b_n^i = \left\{\phi_n^i\right\}^T\left[M_n\right]\left\{y_0\right\}$$

Then

$$\left\{q_n\right\} = \begin{Bmatrix} q_n^1 \\ q_n^2 \\ \vdots \\ q_n^m \end{Bmatrix} \tag{B12}$$

The required result $\left\{y_n\right\}$ is finally obtained by substituting equation (B12) into equation (B3).

APPENDIX C

FINITE-ELEMENT CALCULATION OF AXISYMMETRIC VIBRATION MODES OF A CYLINDER INCLUDING SECONDARY EFFECTS

In figure 2 the displacement components in the meridional and normal directions at a general point in the cylinder cross section are denoted as U and W, respectively. The corresponding displacement components at a point on the middle surface of the cylinder are denoted by u and w, respectively. The rotation of a shell generator is denoted by β. A point is located in the cylinder by the meridional coordinate s, the circumferential coordinate θ, and the normal coordinate z. The middle surface of the shell is taken as the reference surface and is located a distance r from the shell axis. Following the usual convention, the U and W, at any time t, for axisymmetric vibration at frequency ω may be separated into functions of displacement and time as follows:

$$\left.\begin{aligned} U(s,z,t) &= \left[u(s) + z\beta(s)\right]e^{i\omega t} \\ W(s,z,t) &= w(s)e^{i\omega t} \end{aligned}\right\} \tag{C1}$$

The maximum strain energy is

$$V = \frac{1}{2}\iiint \left(\sigma_1 e_1 + \sigma_2 e_2 + \sigma_{13}\gamma_{13}\right) r \, ds \, d\theta \, dz \tag{C2}$$

The strain-displacement relations are

$$\left.\begin{aligned} e_1 &= \frac{\partial U}{\partial s} \\ e_2 &= \frac{W}{r} \\ \gamma_{13} &= \frac{\partial W}{\partial s} + \frac{\partial U}{\partial z} \end{aligned}\right\} \tag{C3}$$

APPENDIX C

The constitutive equations are

$$\left.\begin{aligned} \sigma_1 &= \frac{E}{1 - \nu^2}(e_1 + \nu e_2) \\ \sigma_2 &= \frac{E}{1 - \nu^2}(e_2 + \nu e_1) \\ \sigma_{13} &= k^2 G h \gamma_{13} \end{aligned}\right\} \tag{C4}$$

Using equations (C1), (C3), and (C4) in equation (C2) and performing the integration with respect to the variables θ and z give the following form for the maximum strain energy:

$$V = \pi r \int_s \left\{ C\left[(u')^2 + \frac{2\nu}{r} u'w + \frac{w^2}{r^2}\right] + D(\beta')^2 + k^2 G h\left[w' + \beta\right]^2 \right\} ds \tag{C5}$$

where

$$C = \frac{Eh}{(1 - \nu^2)}$$

and

$$D = \frac{Eh^3}{12(1 - \nu^2)}$$

The integration indicated by $\int_s$ is taken over the cylinder length. The membrane stiffness is C and the flexural stiffness is D. Equation (C5) may be written as a quadratic form as follows:

$$V = \frac{\pi}{2} \int_s \{\delta\}^T [R] \{\delta\} ds \tag{C6}$$

where

$$[R] = \begin{bmatrix} 2Cr & 2\nu C & 0 & 0 & 0 \\ 2\nu C & 2C/r & 0 & 0 & 0 \\ 0 & 0 & 2k^2 Ghr & 0 & 0 \\ 0 & 0 & 0 & 2k^2 Ghr & 0 \\ 0 & 0 & 0 & 0 & 2Dr \end{bmatrix} \tag{C7}$$

APPENDIX C

$$\{\delta\} = \begin{Bmatrix} u' \\ w \\ w' \\ \beta \\ \beta' \end{Bmatrix} \tag{C8}$$

Kinetic Energy

The maximum kinetic energy of a thin cylindrical shell is

$$T = \frac{1}{2}\int\int\int \rho\left[\dot{U}^2 + \dot{W}^2\right] r \, ds \, d\theta \, dz \tag{C9}$$

Substituting equation (C1) into equation (C9) and carrying out the integration with respect to θ and z yield the following result for the maximum kinetic energy:

$$T = \omega^2 \pi \int_s \rho hr\left(u^2 + w^2 + \alpha\beta^2\right) ds \tag{C10}$$

where $\alpha = \frac{h^2}{12}$. Equation (C10) may be written as a quadratic form as follows:

$$T = \frac{\omega^2}{2} \pi \int_s \{\xi\}^T [F] \{\xi\} ds \tag{C11}$$

where

$$[F] = \begin{bmatrix} 2\rho hr & 0 & 0 \\ 0 & 2\rho hr & 0 \\ 0 & 0 & 2\alpha\rho hr \end{bmatrix} \tag{C12}$$

$$\{\xi\} = \begin{Bmatrix} u \\ w \\ \beta \end{Bmatrix} \tag{C13}$$

Representation of Shell Finite Elements

The cylinder is modeled by finite elements as shown in figure 3. Each element is an exact slice of the cylinder being analyzed. The following definitions are made in connection with the finite-element representation:

$\bar{K}$ total number of elements

ϵ_k length of the kth element, $k = 1, 2, \ldots, \bar{K}$

x meridional coordinate inside kth element measured from center of element; thus $-\frac{\epsilon_k}{2} \leqq x \leqq \frac{\epsilon_k}{2}$

s_k distance from first edge of cylinder to center of kth element

From these definitions for x and s_k it follows that

$$s = s_k + x$$

The convention used herein is that quantities such as displacement components and their derivatives at $s = s_k - \frac{\epsilon_k}{2}$ and $s = s_k + \frac{\epsilon_k}{2}$ are denoted by the subscripts k and $k + 1$, respectively. For example, u_k is the meridional displacement at $s = s_k - \frac{\epsilon_k}{2}$ and β'_{k+1} is the derivative of β at $s = s_k + \frac{\epsilon_k}{2}$.

The quantities u, w, and β are approximated over each element by the following polynomials:

$$\left.\begin{aligned} u &= a_{0,k} + a_{1,k}x + a_{2,k}x^2 + a_{3,k}x^3 \\ w &= b_{0,k} + b_{1,k}x + b_{2,k}x^2 + b_{3,k}x^3 \\ \beta &= c_{0,k} + c_{1,k}x + c_{2,k}x^2 + c_{3,k}x^3 \end{aligned}\right\} \tag{C14}$$

Using equations (C8) and (C14) yields

$$\{\delta\} = [X]\{\gamma\} \tag{C15}$$

where

$$\{\gamma\} = \begin{Bmatrix} a_{0,k} \\ a_{1,k} \\ a_{2,k} \\ a_{3,k} \\ b_{0,k} \\ b_{1,k} \\ b_{2,k} \\ b_{3,k} \\ c_{0,k} \\ c_{1,k} \\ c_{2,k} \\ c_{3,k} \end{Bmatrix} \tag{C16}$$

$$[X] = \begin{bmatrix} 0 & 1 & 2x & 3x^2 & 0 & 0 & 0 & 0 & 0 & 0 & 0 & 0 \\ 0 & 0 & 0 & 0 & 1 & x & x^2 & x^3 & 0 & 0 & 0 & 0 \\ 0 & 0 & 0 & 0 & 0 & 1 & 2x & 3x^2 & 0 & 0 & 0 & 0 \\ 0 & 0 & 0 & 0 & 0 & 0 & 0 & 0 & 1 & x & x^2 & x^3 \\ 0 & 0 & 0 & 0 & 0 & 0 & 0 & 0 & 0 & 1 & 2x & 3x^2 \end{bmatrix} \tag{C17}$$

Inserting $x = \frac{-\epsilon_k}{2}$ and $\frac{\epsilon_k}{2}$ into appropriate locations in equation (C17), using equation (C15) with the first of equations (C14), and inverting the resulting equation give

$$\{\gamma\} = [A_k]\{\eta_k\} \tag{C18}$$

where

$$\{\eta_k\} = \begin{Bmatrix} u_k \\ w_k \\ \beta_k \\ u_k' \\ w_k' \\ \beta_k' \\ u_{k+1} \\ w_{k+1} \\ \beta_{k+1} \\ u_{k+1}' \\ w_{k+1}' \\ \beta_{k+1}' \end{Bmatrix}$$

and the elements of $[A_k]$ are

$$[A_k] = \begin{bmatrix}
\frac{1}{2} & 0 & 0 & \frac{\epsilon_k}{8} & 0 & 0 & \frac{1}{2} & 0 & 0 & \frac{-\epsilon_k}{8} & 0 & 0 \\
\frac{-3}{2\epsilon_k} & 0 & 0 & \frac{-1}{4} & 0 & 0 & \frac{3}{2\epsilon_k} & 0 & 0 & \frac{-1}{4} & 0 & 0 \\
0 & 0 & 0 & \frac{-1}{2\epsilon_k} & 0 & 0 & 0 & 0 & 0 & \frac{1}{2\epsilon_k} & 0 & 0 \\
\frac{2}{\epsilon_k^3} & 0 & 0 & \frac{1}{\epsilon_k^2} & 0 & 0 & \frac{-2}{\epsilon_k^3} & 0 & 0 & \frac{1}{\epsilon_k^2} & 0 & 0 \\
0 & \frac{1}{2} & 0 & 0 & \frac{\epsilon_k}{8} & 0 & 0 & \frac{1}{2} & 0 & 0 & \frac{-\epsilon_k}{8} & 0 \\
0 & \frac{-3}{2\epsilon_k} & 0 & 0 & \frac{-1}{4} & 0 & 0 & \frac{3}{2\epsilon_k} & 0 & 0 & \frac{-1}{4} & 0 \\
0 & 0 & 0 & 0 & \frac{-1}{2\epsilon_k} & 0 & 0 & 0 & 0 & 0 & \frac{1}{2\epsilon_k} & 0 \\
0 & \frac{2}{\epsilon_k^3} & 0 & 0 & \frac{1}{\epsilon_k^2} & 0 & 0 & \frac{-2}{\epsilon_k^3} & 0 & 0 & \frac{1}{\epsilon_k^2} & 0 \\
0 & 0 & \frac{1}{2} & 0 & 0 & \frac{\epsilon_k}{8} & 0 & 0 & \frac{1}{2} & 0 & 0 & \frac{-\epsilon_k}{8} \\
0 & 0 & \frac{-3}{2\epsilon_k} & 0 & 0 & \frac{-1}{4} & 0 & 0 & \frac{3}{2\epsilon_k} & 0 & 0 & \frac{-1}{4} \\
0 & 0 & 0 & 0 & 0 & \frac{-1}{2\epsilon_k} & 0 & 0 & 0 & 0 & 0 & \frac{1}{2\epsilon_k} \\
0 & 0 & \frac{2}{\epsilon_k^3} & 0 & 0 & \frac{1}{\epsilon_k^2} & 0 & 0 & \frac{-2}{\epsilon_k^3} & 0 & 0 & \frac{1}{\epsilon_k^2}
\end{bmatrix} \qquad \text{(C19)}$$

APPENDIX C

Formulation of Element Stiffness Matrix

Substitution of equation (C15) into equation (C6) and integration over a single element give

$$V = \frac{1}{2}\{\gamma\}^T[C_k]\{\gamma\} \tag{C20}$$

where

$$[C_k] = \pi \int_{-\epsilon_k/2}^{\epsilon_k/2} [X]^T[R][X]\,dx \tag{C21}$$

The integral in equation (C21) is evaluated numerically by using the trapezoidal rule with 100 integration intervals. Using equation (C18) in equation (C20) gives

$$V = \frac{1}{2}\{\eta_k\}^T[A_k]^T[C_k][A_k]\{\eta_k\} \tag{C22}$$

Thus the element stiffness matrix for the kth element is given by

$$[S_k] = [A_k]^T[C_k][A_k] \tag{C23}$$

Formulation of Element Mass Matrix

Using equations (C13) and (C14) gives

$$\{\xi\} = [Y]\{\gamma\} \tag{C24}$$

where

$$[Y] = \begin{bmatrix} 1 & x & x^2 & x^3 & 0 & 0 & 0 & 0 & 0 & 0 & 0 & 0 \\ 0 & 0 & 0 & 0 & 1 & x & x^2 & x^3 & 0 & 0 & 0 & 0 \\ 0 & 0 & 0 & 0 & 0 & 0 & 0 & 0 & 1 & x & x^2 & x^3 \end{bmatrix} \tag{C25}$$

Substitution of equation (C24) into equation (C11) and integration over a single element yield the following expression for maximum kinetic energy:

$$T = \frac{\omega^2}{2}\{\gamma\}^T[Z_k]\{\gamma\} \tag{C26}$$

where

$$\left[Z_k\right] = \pi \int_{-\epsilon_k/2}^{\epsilon_k/2} \left[Y\right]^T \left[F\right] \left[Y\right] dx \tag{C27}$$

The integral in equation (C27) is evaluated by use of the trapezoidal rule. Using equations (C18) and (C26) gives

$$T = \frac{\omega^2}{2} \left\{\eta_k\right\}^T \left[A_k\right]^T \left[Z_k\right] \left[A_k\right] \left\{\eta_k\right\} \tag{C28}$$

Thus the element mass matrix is given by

$$\left[M_k\right] = \left[A_k\right]^T \left[Z_k\right] \left[A_k\right] \tag{C29}$$

Formulation of Modal Equations

The stiffness and mass matrices for the complete cylinder are synthesized from the corresponding element matrices as described in reference 7. This synthesis is accomplished by superimposing the lower right 6×6 block of the kth matrix and the upper left 6×6 block of the k+1st matrix. The superposition of element matrices is predicted on the following conditions of compatibility at junctures between elements:

$$\begin{Bmatrix} u_{k+1} \\ w_{k+1} \\ \beta_{k+1} \\ u'_{k+1} \\ w'_{k+1} \\ \beta'_{k+1} \end{Bmatrix}_{\text{kth element}} = \begin{Bmatrix} u_{k+1} \\ w_{k+1} \\ \beta_{k+1} \\ u'_{k+1} \\ w'_{k+1} \\ \beta'_{k+1} \end{Bmatrix}_{\text{k+1st element}} \quad \text{for all} \quad k < \bar{K} \tag{C30}$$

By denoting the master stiffness and mass matrices for the shell by $\left[S\right]$ and $\left[M\right]$, respectively, and using the principle of minimum potential energy one obtains

$$\left[S\right]\left\{y\right\} - \omega^2 \left[M\right]\left\{y\right\} = 0 \tag{C31}$$

which is the modal set of equations for the system and where $\left\{y\right\}$ is a $6(\bar{K}+1) \times 1$ vector given by

APPENDIX C

$$\{y\} = \begin{Bmatrix} \eta_1 \\ \eta_2 \\ \cdot \\ \cdot \\ \cdot \\ \eta_k \end{Bmatrix} \tag{C32}$$

The matrices in equation (C31) are modified by deleting rows and columns as necessary to satisfy the specific edge constraints. Equation (C31) is solved by a standard eigenvalue extraction algorithm to yield natural frequencies ω and modal columns $\{y\}$.

Mode Shapes and Modal Stress and Moment Resultants

The modal columns $\{y\}$ contain values of u, w, β, u', w', and β' at the element junctures. In order to obtain a detailed mode shape, the coefficients of the polynomial representations of u, w, and β are obtained by use of equation (C18). Then, by using equation (C14), the mode shapes may be computed within each element and hence over the entire shell.

The modal stress and moment resultants are obtained from the modal strains and displacements. (See appendix B of ref. 8.)

Meridional stress resultant:

$$N_x = C\left(u' + \frac{\nu w}{r}\right) \tag{C33}$$

Meridional moment resultant:

$$M_x = D\beta' \tag{C34}$$

Transverse shear stress resultant:

$$Q_x = k^2 Gh(w' + \beta) \tag{C35}$$

Accuracy of Modal Characteristics

To assess the reliability of the modes supplied by this method, a computer program based on the method was used to calculate mode shapes, frequencies, and modal stresses of a cylinder whose properties are listed below:

APPENDIX C

$L = 63.5$ cm (25 in.)

$r = 25.4$ cm (10 in.)

$h = 1.01$ cm (0.4 in.)

$E = 207\ \mathrm{GN/m^2}\ \left(3 \times 10^7\ \mathrm{lb/in^2}\right)$

$\rho = 7843\ \mathrm{kg/m^3}\ \left(7.33 \times 10^{-4}\ \mathrm{lb\text{-}sec^2/in^4}\right)$

$\nu = 0.30$

$k^2 = 0.87$

Calculations are carried out for clamped-clamped boundaries. Results were compared with those obtained by the more general-purpose computer program (ref. 7). The latter program does not include rotary inertia or transverse shear effects but a satisfactory comparison can be made for the low-frequency modes where effects of rotary inertia and transverse shear deformation are small.

There is a certain amount of difficulty in deciding which modes to compare. For the low-frequency modes, close agreement is observed between the two methods. Because of the differences noted in the two programs, there is not a one-to-one correspondence between modes from each program over the entire frequency spectrum. The following table contains frequency comparisons for the 10 lowest frequencies. The frequencies are in good agreement for those modes, with an increasing disparity evident with increasing mode number. This disparity in the higher frequencies is due to the secondary effects.

COMPARISON OF FREQUENCIES FROM PROGRAM METHOD OF APPENDIX C AND REFERENCE 7 FOR A CLAMPED-CLAMPED CYLINDER

Description of mode	Frequency, Hz (appendix C)	Frequency, Hz (ref. 7)
First w mode	3120.38	3122.17
Second w mode	3259.15	3262.10
Third w mode	3367.92	3370.17
Fourth w mode	3410.42	3420.52
Fifth w mode	3700.37	3722.45
Sixth w mode	4045.63	4085.35
First u mode	4465.32	4472.51
Seventh w mode	4644.45	4725.28
Eighth w mode	5363.40	5497.80
Ninth w mode	6203.20	6414.83

APPENDIX C

Mode shapes and modal stress comparisons for the first five modes are shown in the machine plots in figure 15. On the left side of each frame are results from the present program and on the right are results from the program of reference 7. Since rotary inertia and transverse shear deformation are neglected in reference 7, there are no corresponding plots for the rotation β or the transverse shear resultant Q_x in the right side of the figure. The corresponding curves in the two analyses for the displacements u and w have excellent agreement in mode shape and, further, the maximum values are in agreement through at least two and often three significant figures. Also modal stress and moment resultants are in excellent qualitative agreement. There is agreement of the first significant digit in peak stress and moment resultants between the two programs and in many cases there is agreement through three significant figures.

The oscillations in the plot for Q_x are at locations which correspond to element junctures and are attributed to the fact that continuity of the slope at element junctures of Q_x is not enforced. Cusps are also evident in the meridional stress resultant in the fifth mode for the same reason.

APPENDIX D

TABULAR DATA

Tables I to IX comprise listings of all data contained in the body of the report.

APPENDIX D

TABLE I

DATA PLOTTED IN FIGURE 4 FOR CYLINDER AT TIME =1.20 SEC

N = 0

L/R =2.40

H = .0500

EXACT		DIR INT		MOD SUP	
S/L	W DISP	S/L	W DISP	S/L	W DISP
0.0000	0.000000	0.0000	0.000000	0.0000	.000000
.0100	.130890	.0104	.135972	.0100	.123230
.0200	.257700	.0208	.270025	.0200	.245474
.0300	.381580	.0313	.400230	.0300	.364561
.0400	.502780	.0417	.524646	.0400	.477949
.0500	.615877	.0521	.641326	.0500	.583886
.0600	.717844	.0625	.748341	.0600	.681938
.0700	.811291	.0729	.843823	.0700	.770777
.0800	.895611	.0833	.926019	.0800	.848469
.0900	.964090	.0938	.993359	.0900	.913440
.1000	1.015938	.1042	1.044555	.1000	.965138
.1100	1.055888	.1146	1.078728	.1100	1.004190
.1200	1.082960	.1250	1.095597	.1200	1.030655
.1300	1.091880	.1354	1.095717	.1300	1.044593
.1400	1.085650	.1458	1.080737	.1400	1.046735
.1500	1.070193	.1563	1.053573	.1500	1.038839
.1600	1.046571	.1667	1.018386	.1600	1.023836
.1700	1.015252	.1771	.980244	.1700	1.004532
.1800	.980116	.1875	.944467	.1800	.982871
.1900	.945075	.1979	.915738	.1900	.960563
.2000	.915575	.2083	.897238	.2000	.939787
.2100	.896207	.2188	.890047	.2100	.923622
.2200	.884001	.2292	.893040	.2200	.913941
.2300	.878456	.2396	.903316	.2300	.910017
.2400	.883512	.2500	.917054	.2400	.909999
.2500	.899628	.2604	.930510	.2500	.912660
.2600	.919119	.2708	.940865	.2600	.918421
.2700	.938611	.2813	.946703	.2700	.926491
.2800	.951643	.2917	.948033	.2800	.934312
.2900	.958390	.3021	.945930	.2900	.939288
.3000	.960562	.3125	.941982	.3000	.940423
.3100	.957999	.3229	.937737	.3100	.939391
.3200	.947039	.3333	.934318	.3200	.938046
.3300	.932425	.3438	.932259	.3300	.936989
.3400	.918447	.3542	.931555	.3400	.935930
.3500	.910884	.3646	.931854	.3500	.934033
.3600	.914963	.3750	.932668	.3600	.930924
.3700	.924435	.3854	.933560	.3700	.928474
.3800	.934705	.3958	.934243	.3800	.927999
.3900	.941171	.4063	.934607	.3900	.929542
.4000	.941697	.4167	.934674	.4000	.931959
.4100	.939459	.4271	.934545	.4100	.933449
.4200	.936103	.4375	.934334	.4200	.933583
.4300	.932394	.4479	.934132	.4300	.932939
.4400	.928685	.4583	.933987	.4400	.932363
.4500	.926157	.4688	.933909	.4500	.932472
.4600	.924842	.4792	.933883	.4600	.933005
.4700	.927743	.4896	.933881	.4700	.932876
.4800	.932678	.5000	.933884	.4800	.931949
.4900	.937481			.4900	.930851
.5000	.940135			.5000	.930367

APPENDIX D

TABLE II

DATA FROM FIGURES 5, 6 FOR CYLINDER AT N = 0 AND TIME = 1.2 SEC

L/R = 2.40

H/R = 0.05

	W/R		M-X	
S/L	LINEAR	SEC EFF	LINEAR	SEC EFF
0.0000	0.000000	0.000000	0.	0.
.0104	.135972	.137643	3.1934E-05	3.2218E-05
.0208	.270025	.273384	6.4058E-05	6.4735E-05
.0313	.400230	.405260	9.6456E-05	9.7709E-05
.0417	.524646	.531284	1.2900E-04	1.3097E-04
.0521	.641326	.649437	1.6130E-04	1.6393E-04
.0625	.748341	.757711	1.9268E-04	1.9577E-04
.0729	.843823	.854174	2.2220E-04	2.2609E-04
.0833	.926019	.937009	2.4871E-04	2.5523E-04
.0938	.993359	1.004432	2.7072E-04	2.8311E-04
.1042	1.044555	1.054609	2.8613E-04	3.0647E-04
.1146	1.078728	1.085779	2.9187E-04	3.1685E-04
.1250	1.095597	1.096842	2.8376E-04	3.0215E-04
.1354	1.095717	1.088320	2.5718E-04	2.5267E-04
.1485	1.080737	1.063213	2.0858E-04	1.6833E-04
.1563	1.053573	1.027130	1.3789E-04	6.2092E-05
.1667	1.018386	.987378	5.0530E-05	-4.3294E-05
.1771	.980244	.951254	-4.2020E-05	-1.2389E-04
.1875	.944467	.924248	-1.2406E-04	-1.6387E-04
.1979	.915738	.908876	-1.7978E-04	-1.6076E-04
.2083	.897238	.904555	-1.9831E-04	-1.2468E-04
.2188	.890047	.908427	-1.7757E-04	-7.2789E-05
.2292	.893040	.916664	-1.2541E-04	-2.2302E-05
.2396	.903316	.925727	-5.7206E-05	1.4875E-05
.2500	.917054	.933172	9.0056E-06	3.4206E-05
.2604	.930510	.937889	5.8039E-05	3.7530E-05
.2708	.940865	.939890	8.1640E-05	3.0322E-05
.2813	.946703	.939860	7.9806E-05	1.8765E-05
.2917	.948033	.938698	5.9327E-05	7.6974E-06
.3021	.945930	.937189	3.0394E-05	-2.3200E-07
.3125	.941982	.935846	2.8831E-06	-4.3886E-06
.3229	.937737	.934897	-1.6435E-05	-5.4513E-06
.3333	.934318	.934361	-2.5025E-05	-4.6256E-06
.3438	.932259	.934140	-2.4115E-05	-3.0569E-06
.3542	.931555	.934105	-1.7197E-05	-1.5348E-06
.3646	.931854	.934148	-8.2866E-06	-4.4230E-07
.3750	.932668	.934197	-5.7000E-07	1.5080E-07
.3854	.933560	.934221	4.2506E-06	3.4930E-07
.3958	.934243	.934214	5.9341E-06	3.1260E-07
.4063	.934607	.934182	5.2377E-06	1.8100E-07
.4167	.934674	.934139	3.3174E-06	4.5500E-08
.4271	.934545	.934095	1.2311E-06	-5.1400E-08
.4375	.934334	.934055	-3.3720E-07	-1.0230E-07
.4479	.934132	.934024	-1.1321E-06	-1.1680E-07
.4583	.933987	.934000	-1.2303E-06	-1.1020E-07
.4688	.933909	.933984	-8.8670E-07	-9.5320E-07
.4792	.933883	.933973	-3.9530E-07	-8.0600E-08
.4896	.933881	.933967	7.0000E-10	-7.0700E-08
.5000	.933884	.933965	1.4970E-07	-6.7200E-08

APPENDIX D

TABLE III

DATA FROM FIGURES 7, 8 FOR CYLINDER AT TIME = 1.2 SEC

N = 0

H/R = 0.05

	L/R = 1.2		L/R = 0.3	
S/L	LINEAR	SEC EFF	LINEAR	SEC EFF
0.0000	0.000000	0.000000	0.000000	0.000000
.0104	.068162	.069017	.018187	.018883
.0208	.136087	.137800	.036356	.037758
.0313	.203534	.206104	.054490	.056603
.0417	.270266	.273689	.072571	.075406
.0521	.336042	.340311	.090583	.094150
.0625	.400621	.405722	.108507	.112822
.0729	.463760	.469673	.126326	.131407
.0833	.525216	.531908	.144022	.149889
.0938	.584746	.592170	.161578	.168253
.1042	.642105	.650202	.178977	.186484
.1146	.697051	.705753	.196200	.204565
.1250	.749343	.758580	.213231	.222481
.1354	.798744	.808454	.230052	.240215
.1458	.845024	.855157	.246646	.257750
.1563	.887956	.898480	.262996	.275068
.1667	.927326	.938207	.279083	.292153
.1771	.962932	.974104	.294892	.308987
.1875	.994584	1.005915	.310405	.325552
.1979	1.022116	1.033352	.325605	.341828
.2083	1.045385	1.056118	.340475	.357798
.2188	1.064279	1.073924	.355000	.373443
.2292	1.078729	1.086535	.369162	.388744
.2396	1.088718	1.093815	.382945	.403680
.2500	1.094287	1.095772	.396333	.418233
.2604	1.095556	1.092597	.409311	.432384
.2708	1.092729	1.084686	.421863	.446113
.2813	1.086103	1.072643	.433975	.459400
.2917	1.076075	1.057254	.445631	.472226
.3021	1.063139	1.039447	.456818	.484572
.3125	1.047879	1.020234	.467522	.496419
.3229	1.030951	1.000638	.477728	.507748
.3333	1.013063	.981629	.487425	.518542
.3438	.994938	.964058	.496600	.528782
.3542	.977283	.948606	.505242	.538450
.3646	.960750	.935756	.513338	.547531
.3750	.945893	.925774	.520879	.556009
.3854	.933142	.918718	.527854	.563868
.3958	.922772	.914454	.534255	.571095
.4063	.914890	.912689	.540073	.577675
.4167	.909434	.913015	.545299	.583597
.4271	.906188	.914946	.549928	.588850
.4375	.904799	.917959	.553952	.593423
.4479	.904822	.921537	.557367	.597308
.4583	.905763	.925196	.560167	.600497
.4688	.907125	.928511	.562349	.602984
.4792	.908461	.931135	.563910	.604764
.4896	.909415	.932814	.564847	.605833
.5000	.909759	.933391	.565159	.606190

APPENDIX D

TABLE IV

DATA FROM FIGURE 9 FOR CYLINDER AT TIME = 2.4 SEC AND N = 0

L/R = 2.40

H/R = 0.050

EXACT		NONLINEAR		SEC EFF	
S/L	W DISP	S/L	W DISP	S/L	W DISPL
0.0000	0.000000	0.0000	0.000000	0.0000	0.000000
.0104	.052062	.0104	.063265	.0104	.052276
.0208	.104591	.0208	.135995	.0208	.105078
.0313	.158016	.0313	.224706	.0313	.158870
.0417	.212681	.0417	.331067	.0417	.214037
.0521	.268811	.0521	.450772	.0521	.270835
.0625	.326483	.0625	.573600	.0625	.329357
.0729	.385594	.0729	.685894	.0729	.389502
.0833	.445845	.0833	.775264	.0833	.450954
.0938	.506730	.0938	.834951	.0938	.513169
.1042	.567538	.1042	.865117	.1042	.575373
.1146	.627363	.1146	.870973	.1146	.636575
.1250	.685130	.1250	.859836	.1250	.695592
.1354	.739632	.1354	.838793	.1354	.751088
.1458	.789576	.1458	.813447	.1458	.801629
.1563	.833652	.1563	.787543	.1563	.845755
.1667	.870597	.1667	.763175	.1667	.882065
.1771	.899279	.1771	.741242	.1771	.909311
.1875	.918783	.1875	.721925	.1875	.926501
.1979	.928494	.1979	.705054	.1979	.933001
.2083	.928180	.2083	.690343	.2083	.928618
.2188	.918059	.2188	.677528	.2188	.913676
.2292	.898844	.2292	.666423	.2292	.889075
.2396	.871770	.2396	.656943	.2396	.856336
.2500	.838566	.2500	.649093	.2500	.817635
.2604	.801404	.2604	.642938	.2604	.775796
.2708	.762782	.2708	.638567	.2708	.734201
.2813	.725375	.2813	.636057	.2813	.696545
.2917	.691833	.2917	.635436	.2917	.666418
.3021	.664555	.3021	.636661	.3021	.646740
.3125	.645452	.3125	.639582	.3125	.639159
.3229	.635726	.3229	.643873	.3229	.643595
.3333	.635695	.3333	.648915	.3333	.658113
.3438	.644704	.3438	.653689	.3438	.679215
.3542	.661149	.3542	.656834	.3542	.702530
.3646	.682620	.3646	.657054	.3646	.723737
.3750	.706181	.3750	.653852	.3750	.739463
.3854	.728730	.3854	.648231	.3854	.747901
.3958	.747416	.3958	.642756	.3958	.749009
.4063	.760023	.4063	.640558	.4063	.744248
.4167	.765269	.4167	.643533	.4167	.735996
.4271	.762957	.4271	.650775	.4271	.726826
.4375	.753966	.4375	.658455	.4375	.718863
.4479	.740072	.4479	.661568	.4479	.713380
.4583	.723656	.4583	.656695	.4583	.710683
.4688	.707336	.4688	.644109	.4688	.710261
.4792	.693599	.4792	.627941	.4792	.711122
.4896	.684473	.4896	.614442	.4896	.712185
.5000	.681278	.5000	.609195	.5000	.712639

APPENDIX D

TABLE V

DATA FROM FIGURES 10, 11 FOR CYLINDER AT TIME = 2.4 SEC

N = 0

L/R = 2.40

	H/R = 0.025		H/R = 0.0125	
S/L	LINEAR	NONLINEAR	LINEAR	NONLINEAR
0.0000	0.000000	0.000000	0.000000	0.000000
.0104	.074326	.112469	.106086	.174000
.0208	.149920	.250327	.215448	.402987
.0313	.227821	.419098	.330139	.646568
.0417	.308629	.597629	.449960	.808619
.0521	.392323	.747703	.571801	.851468
.0625	.478139	.838337	.689544	.821327
.0729	.564507	.865831	.794634	.776025
.0833	.649073	.849797	.877391	.739095
.0938	.728817	.814626	.928953	.711846
.1042	.800265	.776969	.943590	.691380
.1146	.859801	.744190	.920900	.675737
.1250	.904060	.717797	.867231	.664065
.1354	.930372	.696898	.795642	.656204
.1458	.937220	.680151	.723852	.652114
.1563	.924637	.666500	.670132	.651206
.1667	.894495	.655340	.647881	.652209
.1771	.850592	.646466	.660553	.653916
.1875	.798474	.639978	.699343	.655989
.1979	.744951	.636134	.745655	.658695
.2083	.697281	.635137	.778600	.661843
.2188	.662079	.636876	.784734	.664375
.2292	.644094	.640696	.764855	.665470
.2396	.645082	.645440	.733195	.665995
.2500	.663126	.649840	.708589	.667506
.2604	.692718	.653181	.702876	.668836
.2708	.725827	.655739	.714384	.666747
.2813	.753843	.658336	.730994	.663508
.2917	.769943	.660906	.740028	.667724
.3021	.771100	.661420	.737050	.678770
.3125	.758946	.657308	.727117	.679314
.3229	.739043	.649331	.718763	.660350
.3333	.718749	.643782	.716782	.644581
.3438	.704483	.648524	.719748	.659247
.3542	.699534	.664637	.723052	.691180
.3646	.703271	.682003	.723529	.700960
.3750	.712022	.685437	.721424	.678105
.3854	.721055	.667779	.718945	.646915
.3958	.726669	.638061	.717740	.628493
.4063	.727465	.616437	.717784	.629406
.4167	.724359	.619008	.718097	.648845
.4271	.719605	.645107	.717957	.677308
.4375	.715480	.678224	.717389	.700847
.4479	.713327	.698329	.716805	.707927
.4583	.713294	.694345	.716476	.694117
.4688	.714670	.668813	.716365	.666786
.4792	.716467	.633988	.716316	.636958
.4896	.717861	.604850	.716258	.611738
.5000	.718375	.593539	.716228	.601029

APPENDIX D

TABLE VI

DATA FROM FIGURE 12 FOR CYLINDER AT N = 2 AND TIME = 2.4 SEC

L/R = 2.40

H/R = 0.05

MODAL		DIRECT	
S/L	LINEAR	S/L	LINEAR
0.0000	.000000	0.0000	-.000000
.0100	.110069	.0052	.057667
.0200	.220853	.0156	.173063
.0300	.332183	.0260	.288625
.0400	.443397	.0365	.404408
.0500	.553961	.0469	.520385
.0600	.663900	.0573	.636420
.0700	.773125	.0677	.752239
.0800	.881105	.0781	.867417
.0900	.987186	.0885	.981360
.1000	1.090911	.0990	1.093302
.1100	1.191703	.1094	1.202311
.1200	1.287683	.1198	1.307305
.1300	1.378048	.1302	1.407073
.1400	1.462927	.1406	1.500323
.1500	1.542430	.1510	1.585723
.1600	1.615423	.1615	1.661973
.1700	1.679213	.1719	1.727869
.1800	1.732228	.1823	1.782390
.1900	1.774241	.1927	1.824779
.2000	1.805987	.2031	1.854628
.2100	1.828787	.2135	1.871954
.2200	1.843666	.2240	1.877264
.2300	1.850644	.2344	1.871593
.2400	1.849569	.2448	1.856524
.2500	1.841163	.2552	1.834172
.2600	1.827602	.2656	1.807121
.2700	1.811071	.2760	1.778317
.2800	1.793651	.2865	1.750893
.2900	1.777222	.2969	1.727918
.3000	1.763097	.3073	1.712079
.3100	1.751581	.3177	1.705328
.3200	1.742742	.3281	1.708547
.3300	1.738163	.3385	1.721327
.3400	1.739855	.3490	1.741925
.3500	1.748663	.3594	1.767480
.3600	1.762783	.3698	1.794459
.3700	1.779201	.3802	1.819278
.3800	1.796722	.3906	1.838952
.3900	1.815139	.4010	1.851614
.4000	1.833819	.4115	1.856775
.4100	1.850103	.4219	1.855266
.4200	1.860021	.4323	1.848873
.4300	1.862291	.4427	1.839814
.4400	1.858081	.4531	1.830194
.4500	1.849928	.4635	1.821605
.4600	1.840083	.4740	1.814963
.4700	1.828884	.4844	1.810589
.4800	1.817606	.4948	1.808454
.4900	1.808673	.5000	1.808454
.5000	1.805036		

APPENDIX D

TABLE VII

DATA FROM FIGURE 13A FOR CYLINDER AT N= 0

L/R = 2.4

H/R = 0.10

LINEAR		SEC EFF		NONLINEAR	
TIME	W-MAX	TIME	W-MAX	TIME	W-MAX
0.0000	0.000000	0.0000	0.000000	0.0000	0.000000
.1000	.107519	.1000	.100648	.1000	.104346
.2000	.215949	.2000	.203263	.2000	.203334
.3000	.328021	.3000	.309262	.3000	.300908
.4000	.438330	.4000	.416733	.4000	.394365
.5000	.544708	.5000	.522937	.5000	.483585
.6000	.647014	.6000	.625444	.6000	.567785
.7000	.742572	.7000	.722552	.7000	.646371
.8000	.830545	.8000	.813057	.8000	.718636
.9000	.910239	.9000	.895943	.9000	.783986
1.0000	.981036	1.0000	.970272	1.0000	.842270
1.1000	1.042389	1.1000	1.035228	1.1000	.891846
1.2000	1.093823	1.2000	1.090157	1.2000	.931921
1.3000	1.135194	1.3000	1.134572	1.3000	.962023
1.4000	1.166994	1.4000	1.168132	1.4000	.982065
1.5000	1.187990	1.5000	1.190622	1.5000	.991570
1.6000	1.197978	1.6000	1.201952	1.6000	.990527
1.7000	1.196964	1.7000	1.202158	1.7000	.978762
1.8000	1.185464	1.8000	1.191402	1.8000	.963455
1.9000	1.165167	1.9000	1.171299	1.9000	.956173
2.0000	1.135928	2.0000	1.140870	2.0000	.943894
2.1000	1.096791	2.1000	1.100602	2.1000	.926687
2.2000	1.045421	2.2000	1.051130	2.2000	.903616
2.3000	.982919	2.3000	.993176	2.3000	.876775
2.4000	.908478	2.4000	.927812	2.4000	.848017

APPENDIX D

TABLE VIII

DATA FROM FIGURE 13B FOR CYLINDER AT N= 0

L/R = 2.4

H/R = 0.10

LINEAR		SEC EFF		NONLINEAR	
TIME	W-L/2	TIME	W-L/2	TIME	W-L/2
0.0000	0.000000	0.0000	0.000000	0.0000	0.000000
.1000	.099834	.1000	.099834	.1000	.099834
.2000	.198674	.2000	.198674	.2000	.198674
.3000	.295540	.3000	.295540	.3000	.295540
.4000	.389471	.4000	.389471	.4000	.389471
.5000	.479540	.5000	.479537	.5000	.479538
.6000	.564868	.6000	.564847	.6000	.564844
.7000	.644629	.7000	.644556	.7000	.644539
.8000	.717986	.8000	.717875	.8000	.717829
.9000	.783986	.9000	.784082	.9000	.783986
1.0000	.841564	1.0000	.842523	1.0000	.842270
1.1000	.889945	1.1000	.892629	1.1000	.891846
1.2000	.929353	1.2000	.933923	1.2000	.931921
1.3000	.961424	1.3000	.966042	1.3000	.962023
1.4000	.988579	1.4000	.988763	1.4000	.981972
1.5000	1.012323	1.5000	1.002056	1.5000	.991569
1.6000	1.031492	1.6000	1.006125	1.6000	.990527
1.7000	1.041782	1.7000	1.001421	1.7000	.978762
1.8000	1.037093	1.8000	.988570	1.8000	.956608
1.9000	1.011992	1.9000	.968145	1.9000	.924782
2.0000	.963914	2.0000	.940311	2.0000	.884215
2.1000	.894069	2.1000	.904440	2.1000	.835971
2.2000	.806857	2.2000	.858910	2.2000	.781362
2.3000	.708391	2.3000	.801310	2.3000	.722376
2.4000	.604917	2.4000	.729167	2.4000	.662495

APPENDIX D

TABLE IX

DATA FROM FIGURE 14 FOR CONICAL SHELL

TIME = 20.E-06 SEC

N = 2

MODAL		DIRECT	
S/L	LINEAR	S/L	LINEAR
0.0000	-1.262079E-19	0.0000	3.183232E-19
.0050	-3.657528E-06	.0051	-1.446202E-05
.0100	-7.544286E-06	.0152	-1.977823E-05
.0150	-1.163078E-05	.0253	-1.873338E-05
.0200	-1.546330E-05	.0354	-1.850952E-05
.0250	-1.824325E-05	.0455	-1.840174E-05
.0300	-1.924761E-05	.0556	-1.826713E-05
.0350	-1.903205E-05	.0657	-1.812024E-05
.0400	-1.848854E-05	.0758	-1.796575E-05
.0450	-1.824199E-05	.0859	-1.780554E-05
.0500	-1.834381E-05	.0960	-1.764081E-05
.0550	-1.830680E-05	.1061	-1.747233E-05
.0600	-1.819370E-05	.1162	-1.730067E-05
.0650	-1.811597E-05	.1263	-1.712625E-05
.0700	-1.806016E-05	.1364	-1.694938E-05
.0750	-1.798296E-05	.1465	-1.677033E-05
.0800	-1.789206E-05	.1566	-1.658929E-05
.0850	-1.781236E-05	.1667	-1.640647E-05
.0900	-1.774018E-05	.1768	-1.622204E-05
.0950	-1.766105E-05	.1869	-1.603614E-05
.1000	-1.757116E-05	.1970	-1.584893E-05
.1050	-1.748581E-05	.2071	-1.566052E-05
.1100	-1.740326E-05	.2172	-1.547103E-05
.1150	-1.732003E-05	.2273	-1.528057E-05
.1200	-1.723582E-05	.2374	-1.508923E-05
.1250	-1.714884E-05	.2475	-1.489709E-05
.1300	-1.705702E-05	.2576	-1.470421E-05
.1350	-1.696895E-05	.2677	-1.451068E-05
.1400	-1.688497E-05	.2778	-1.431654E-05
.1450	-1.679891E-05	.2879	-1.412186E-05
.1500	-1.670676E-05	.2980	-1.392667E-05
.1550	-1.661334E-05	.3081	-1.373102E-05
.1600	-1.652383E-05	.3182	-1.353494E-05
.1650	-1.643685E-05	.3283	-1.333848E-05
.1700	-1.634807E-05	.3384	-1.314167E-05
.1750	-1.625449E-05	.3485	-1.294452E-05
.1800	-1.615899E-05	.3586	-1.274707E-05
.1850	-1.606744E-05	.3687	-1.254934E-05
.1900	-1.597872E-05	.3788	-1.235135E-05
.1950	-1.588804E-05	.3889	-1.215313E-05
.2000	-1.579261E-05	.3990	-1.195468E-05
.2050	-1.569611E-05	.4091	-1.175602E-05
.2100	-1.560281E-05	.4192	-1.155717E-05
.2150	-1.551196E-05	.4293	-1.135815E-05
.2200	-1.542028E-05	.4394	-1.115896E-05
.2250	-1.532507E-05	.4495	-1.095961E-05
.2300	-1.522733E-05	.4596	-1.076013E-05
.2350	-1.512943E-05	.4697	-1.056050E-05
.2400	-1.503126E-05	.4798	-1.036075E-05
.2450	-1.493677E-05	.4899	-1.016089E-05
.2500	-1.486208E-05	.5000	-9.960909E-06

APPENDIX D

TABLE IX CONCL

DATA FROM FIGURE 14 FOR CONICAL SHELL

TIME = 20.E-06 SEC

N = 2

MODAL		DIRECT	
S/L	LINEAR	S/L	LINEAR
.2600	-1.477102E-05	.5101	-9.760828E-06
.2700	-1.454188E-05	.5202	-9.560650E-06
.2800	-1.420230E-05	.5303	-9.360381E-06
.2900	-1.395122E-05	.5404	-9.160027E-06
.3000	-1.388975E-05	.5505	-8.959592E-06
.3100	-1.382045E-05	.5606	-8.759081E-06
.3200	-1.357086E-05	.5707	-8.558499E-06
.3300	-1.323129E-05	.5808	-8.357850E-06
.3400	-1.298519E-05	.5909	-8.157137E-06
.3500	-1.291485E-05	.6010	-7.956364E-06
.3600	-1.284515E-05	.6111	-7.755535E-06
.3700	-1.259658E-05	.6212	-7.554652E-06
.3800	-1.225389E-05	.6313	-7.353719E-06
.3900	-1.200520E-05	.6414	-7.152737E-06
.4000	-1.193542E-05	.6515	-6.951711E-06
.4100	-1.186412E-05	.6616	-6.750641E-06
.4200	-1.161403E-05	.6717	-6.549531E-06
.4300	-1.127076E-05	.6818	-6.348382E-06
.4400	-1.102091E-05	.6919	-6.147196E-06
.4500	-1.094955E-05	.7020	-5.945976E-06
.4600	-1.087880E-05	.7121	-5.744722E-06
.4700	-1.062813E-05	.7222	-5.543437E-06
.4800	-1.028198E-05	.7323	-5.342122E-06
.4900	-1.002970E-05	.7424	-5.140779E-06
.5000	-9.961797E-06	.7525	-4.939408E-06
.5200	-9.842923E-06	.7626	-4.738011E-06
.5400	-9.333085E-06	.7727	-4.536590E-06
.5600	-8.607981E-06	.7828	-4.335146E-06
.5800	-8.091130E-06	.7929	-4.133679E-06
.6000	-7.977379E-06	.8030	-3.932190E-06
.6200	-7.860464E-06	.8131	-3.730681E-06
.6400	-7.343787E-06	.8232	-3.529153E-06
.6600	-6.619221E-06	.8333	-3.327606E-06
.6800	-6.103482E-06	.8434	-3.126041E-06
.7000	-5.985991E-06	.8535	-2.924460E-06
.7200	-5.869312E-06	.8636	-2.722862E-06
.7400	-5.352816E-06	.8737	-2.521248E-06
.7600	-4.626548E-06	.8838	-2.319619E-06
.7800	-4.109890E-06	.8939	-2.117976E-06
.8000	-3.992979E-06	.9040	-1.916320E-06
.8200	-3.875073E-06	.9141	-1.714651E-06
.8400	-3.358155E-06	.9242	-1.512969E-06
.8600	-2.632091E-06	.9343	-1.311275E-06
.8800	-2.114320E-06	.9444	-1.109570E-06
.9000	-1.996420E-06	.9545	-9.078537E-07
.9200	-1.880537E-06	.9646	-7.061278E-07
.9400	-1.361560E-06	.9747	-5.043900E-07
.9600	-8.342620E-07	.9848	-3.026221E-07
.9800	-1.196191E-07	.9949	-1.009266E-07
1.0000	1.167211E-08	1.0000	-3.992516E-10

REFERENCES

1. Stephens, Wendell B.: Computer Program for Static and Dynamic Axisymmetric Nonlinear Response of Symmetrically Loaded Orthotropic Shells of Revolution. NASA TN D-6158, 1970.

2. Stephens, Wendell B.; and Fulton, Robert E.: Axisymmetric Static and Dynamic Buckling of Spherical Caps Due to Centrally Distributed Pressures. AIAA J., vol. 7, no. 11, Nov. 1969, pp. 2120-2126.

3. Stephens, Wendell B.; and Robinson, Martha P.: Computer Program for Finite-Difference Solutions of Shells of Revolution Under Asymmetric Dynamic Loading. NASA TN D-6059, 1971.

4. Johnson, Donald E.; and Greif, Robert: Dynamic Response of a Cylindrical Shell: Two Numerical Methods. AIAA J., vol. 4, no. 3, Mar. 1966, pp. 486-494.

5. Geers, Thomas L.; and Sobel, Lawrence H.: Analysis of Transient, Linear Wave Propagation in Shells by the Finite Difference Method. NASA CR-1885, 1971.

6. Raney, J. P.; and Howlett, J. T.: A Modal Solution for Wave Propagation in Finite Shells of Revolution. J. Spacecraft & Rockets, vol. 8, no. 6, June 1971, pp. 650-656.

7. Adelman, Howard M.; Catherines, Donnell S.; and Walton, William C., Jr.: A Method for Computation of Vibration Modes and Frequencies of Orthotropic Thin Shells of Revolution Having General Meridional Curvature. NASA TN D-4972, 1969.

8. Adelman, Howard M.; Catherines, Donnell S.; Steeves, Earl E.; and Walton, William C., Jr.: User's Manual for a Digital Computer Program for Computing the Vibration Characteristics of Ring-Stiffened Orthotropic Shells of Revolution. NASA TM X-2138, 1970.

9. MacNeal, Richard H., ed.: The NASTRAN Theoretical Manual (Level 15). NASA SP-221(01), 1972.

10. Almroth, B. O.; Brogan, F. A.; and Marlowe, M. B.: Collapse Analysis for Shells of General Shape. Volume 1 – Analysis. AFFDL-TR-71-8, U.S. Air Force, Aug. 1972.

11. Sanders, J. Lyell, Jr.: Nonlinear Theories for Thin Shells. Quart. Appl. Math., vol. XXI, no. 1, Apr. 1963, pp. 21-36.

12. Heard, Walter L., Jr.; Anderson, Melvin S.; Anderson, James Kent; and Card, Michael F.: Design, Analysis, and Tests of a Structural Prototype Viking Aeroshell. J. Spacecraft & Rockets, vol. 10, no. 1, Jan. 1973, pp. 56-65.

13. Adelman, Howard M.; Lester, Harold C.; and Rogers, James L., Jr.: A Finite Element for Thermal Stress Analysis of Shells of Revolution. NASA TN D-7286, 1973.

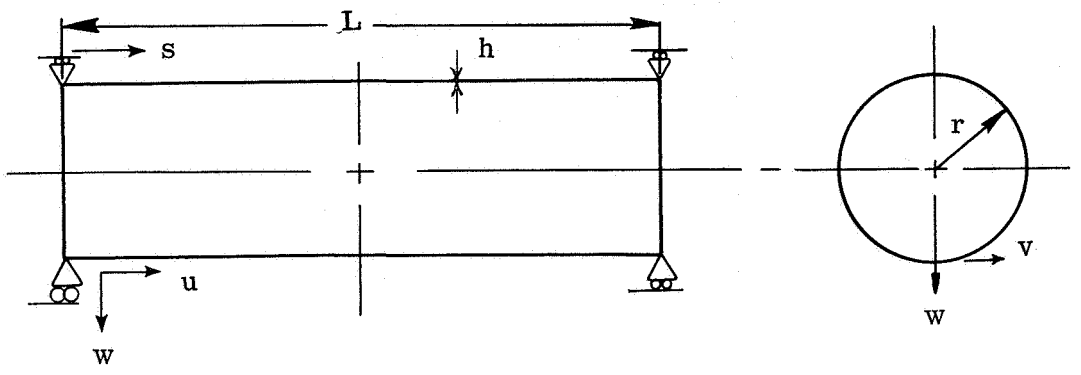

(a) Cylindrical shell.

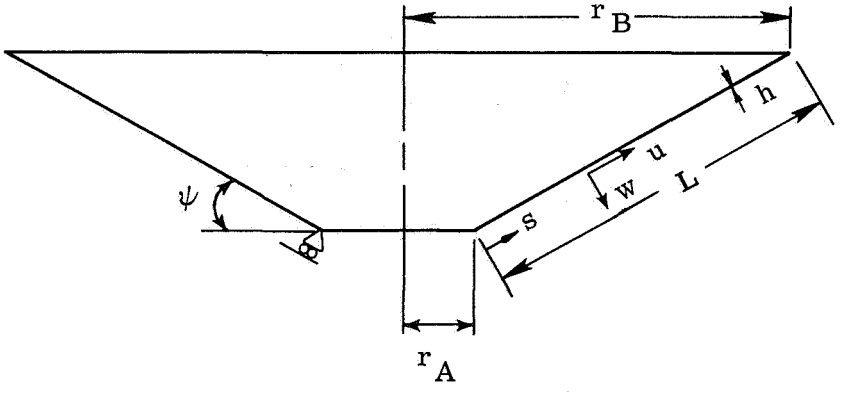

(b) Conical shell.

Figure 1.- Geometry and sign convention for shells used in sample calculations.

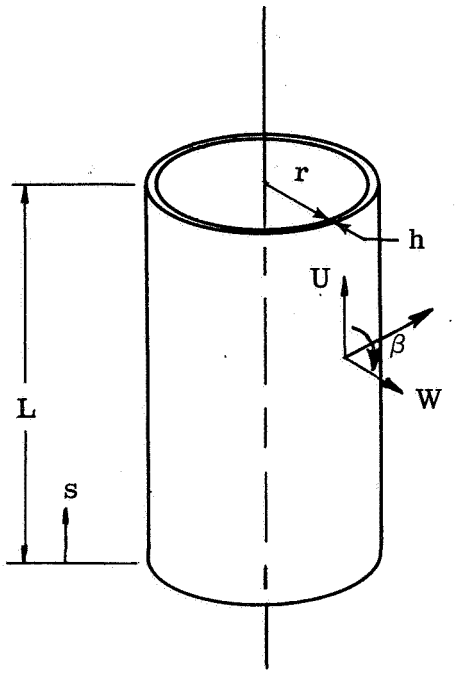

(a) Geometry of cylindrical shell.

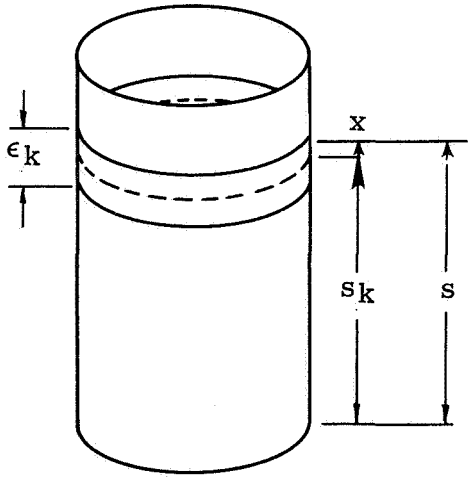

(b) Nomenclature associated with finite-element representation of cylindrical shell.

Figure 2.- Geometry and nomenclature of finite-element model.

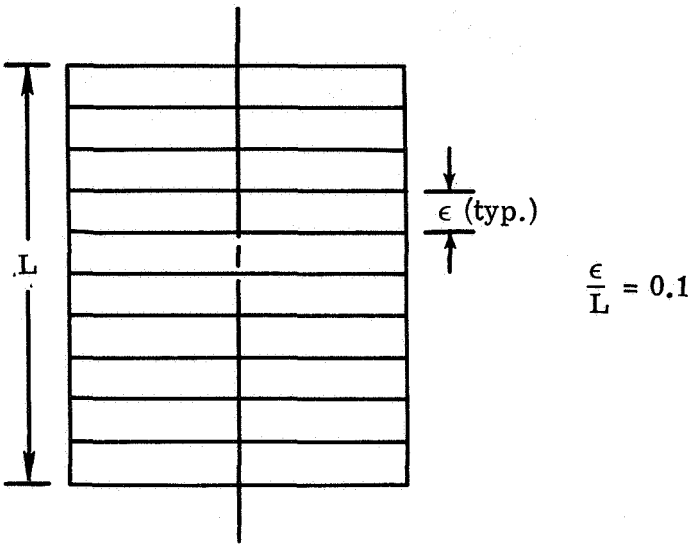

(a) Cylindrical shell representation by 10 equally spaced elements.

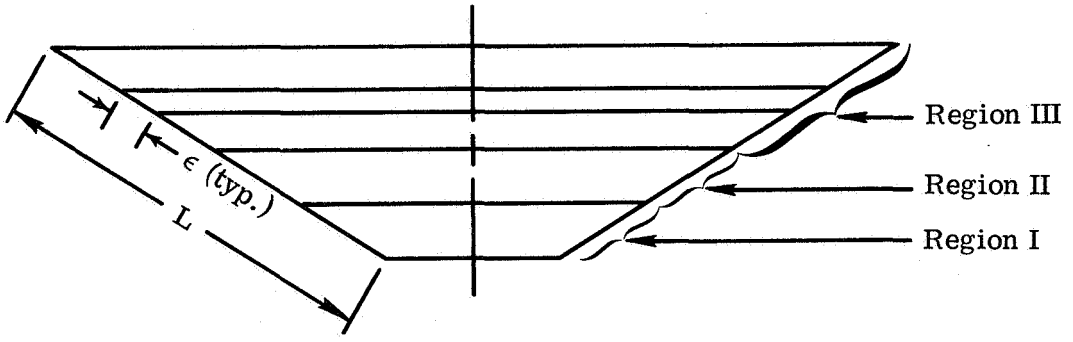

Region I: ten elements - $\epsilon/L = .025$
Region II: five elements - $\epsilon/L = .050$
Region III: five elements - $\epsilon/L = .100$

(b) Conical shell representation by 20 unequally spaced elements.

Figure 3.- Finite-element representations of shells.

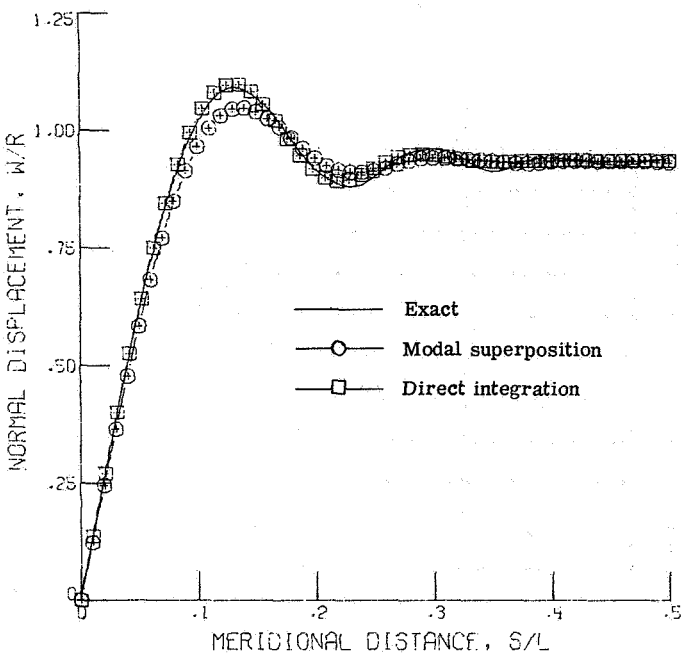

Figure 4.- Comparison of methods at $n = 0$ and $t = 1.2$ sec for a cylindrical shell having $L/r = 2.4$ and $h/r = 0.05$.

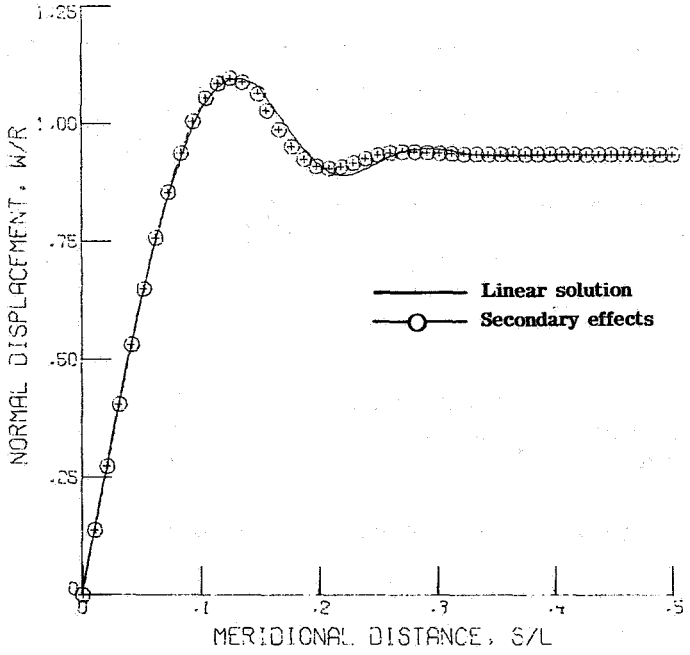

Figure 5.- Effects of rotary inertia and transverse shear deformation on displacement at $n = 0$ and $t = 1.2$ sec for a cylindrical shell having $L/r = 2.4$ and $h/r = 0.05$.

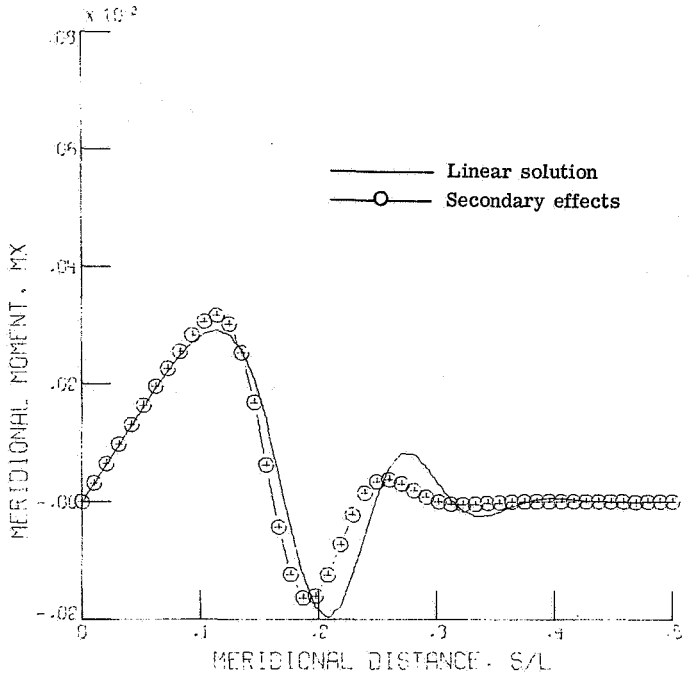

Figure 6.- Effects of rotary inertia and transverse shear deformation on meridional moment resultant at $n = 0$ and $t = 1.2$ sec for a cylindrical shell having $L/r = 2.4$ and $h/r = 0.05$. $\left(MX = M_x/(\rho v_o{}^2 r^2).\right)$

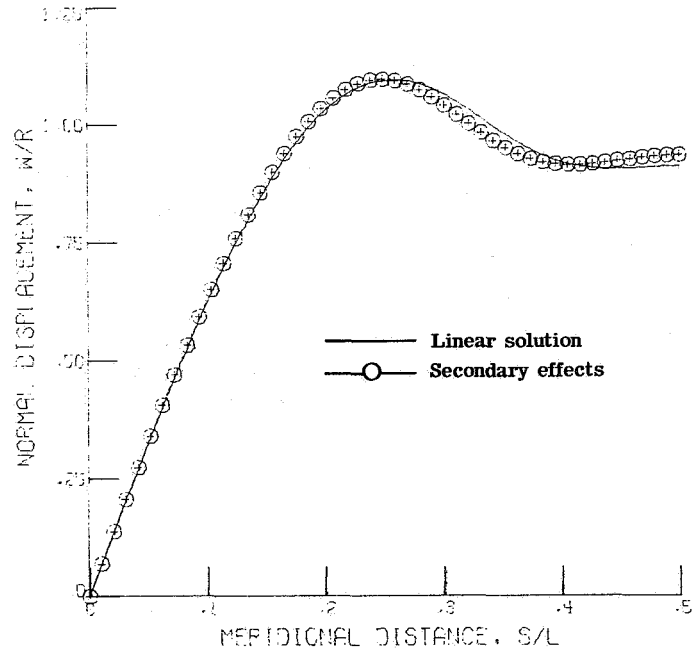

Figure 7.- Effects of rotary inertia and transverse shear deformation on displacement at $n = 0$ and $t = 1.2$ sec for a cylindrical shell having $L/r = 1.2$ and $h/r = 0.05$.

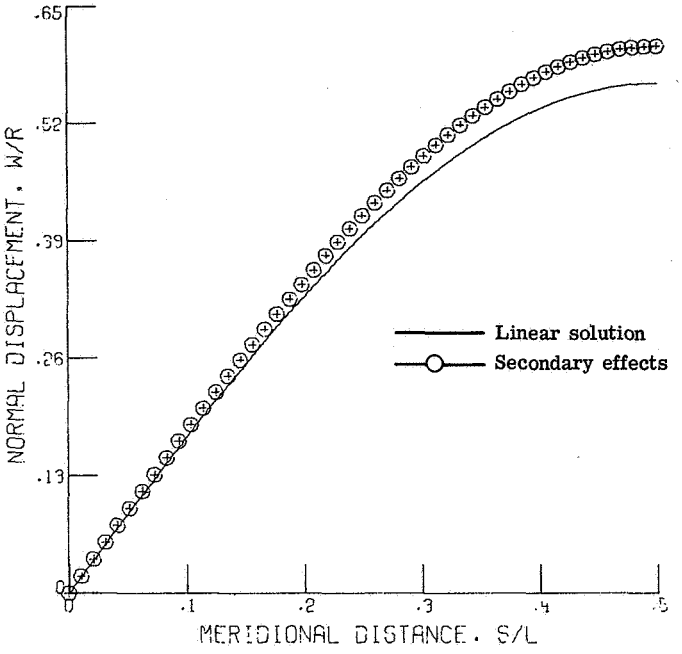

Figure 8.- Effects of rotary inertia and transverse shear deformation on displacement at $n = 0$ and $t = 1.2$ sec for a cylindrical shell having $L/r = 0.3$ and $h/r = 0.05$.

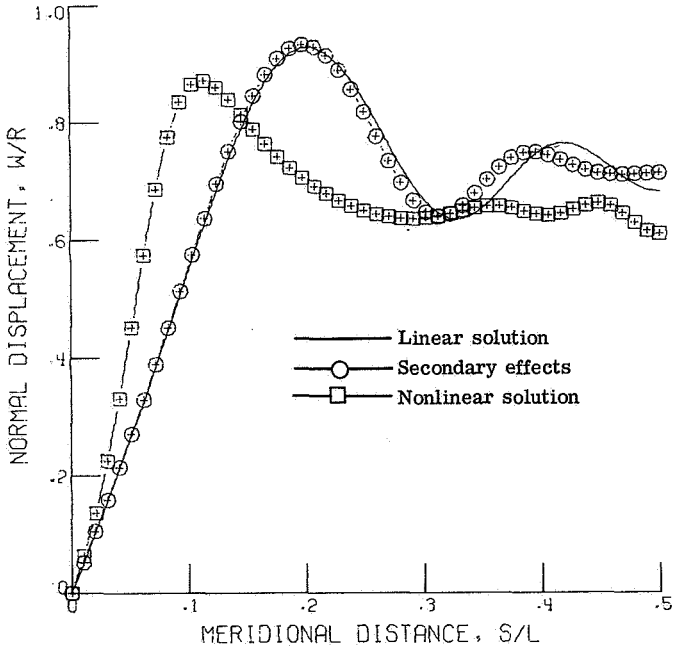

Figure 9.- Comparison of higher order effects on displacement at $n = 0$ and $t = 2.4$ sec for a cylindrical shell having $L/r = 2.4$ and $h/r = 0.05$.

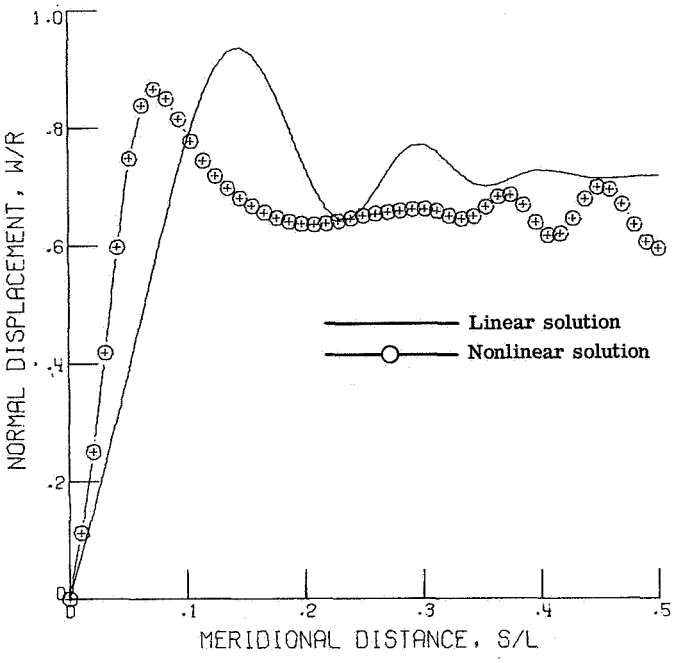

Figure 10.- Effect of nonlinearities on displacement at $n = 0$ and $t = 2.4$ sec for a cylindrical shell having $L/r = 2.4$ and $h/r = 0.025$.

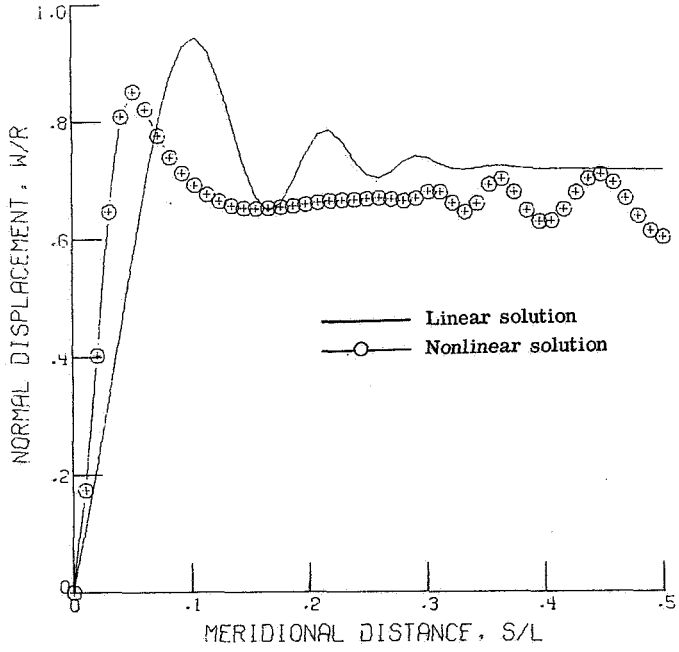

Figure 11.- Effect of nonlinearities on displacement at $n = 0$ and $t = 2.4$ sec for a cylindrical shell having $L/r = 2.4$ and $h/r = 0.0125$.

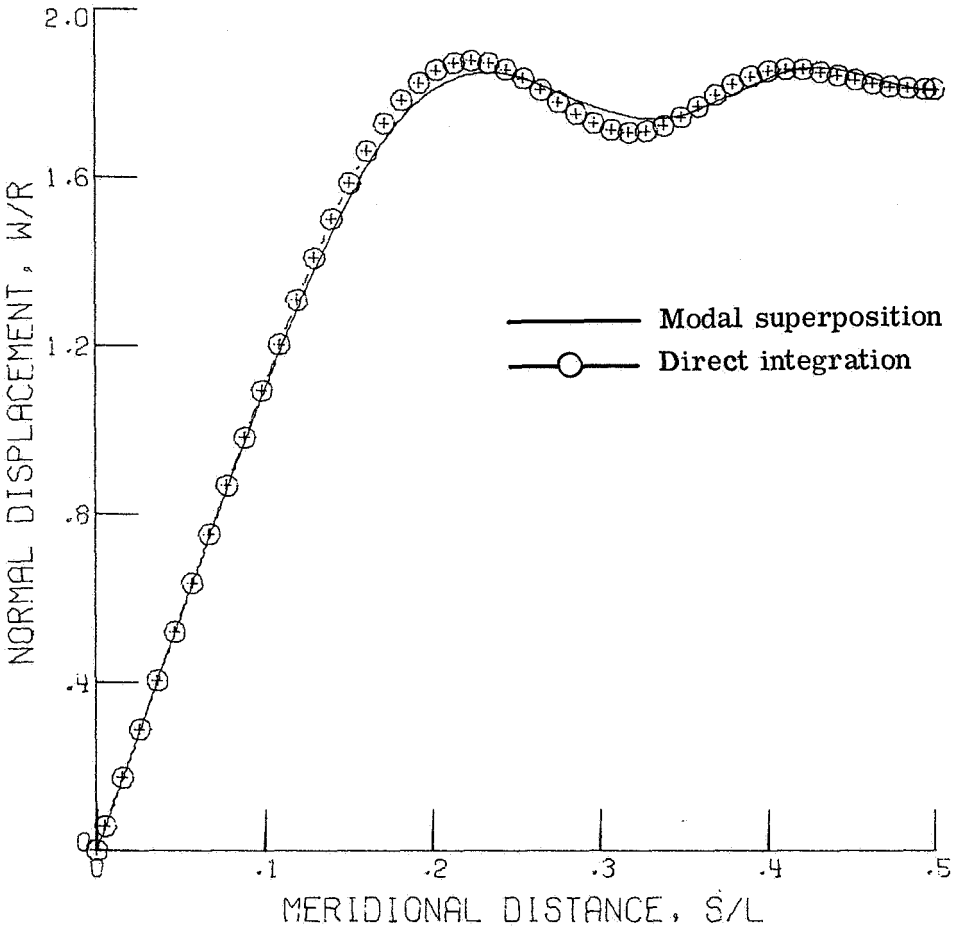

Figure 12.- Comparison of methods at $n = 2$ and $t = 2.4$ sec for a cylindrical shell having $L/r = 2.4$ and $h/r = 0.05$.

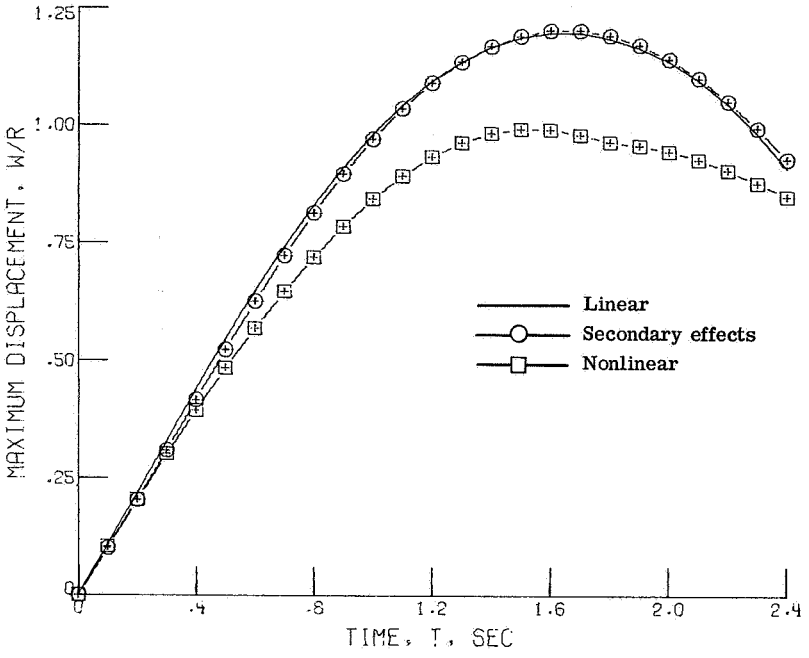

(a) Maximum displacement.

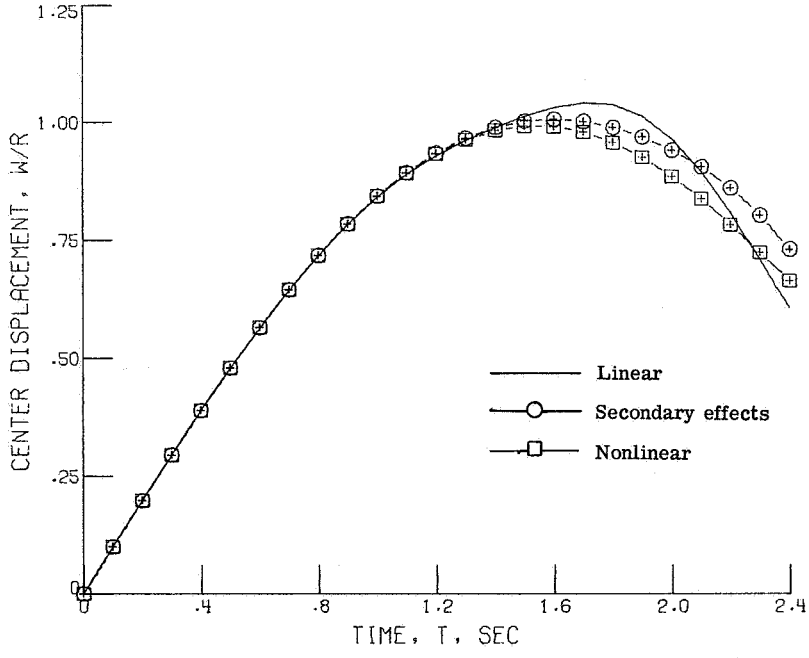

(b) Displacement at L/2.

Figure 13.- Displacement at n = 0 as a function of time for cylinder having L/r = 2.4 and h/r = 0.10.

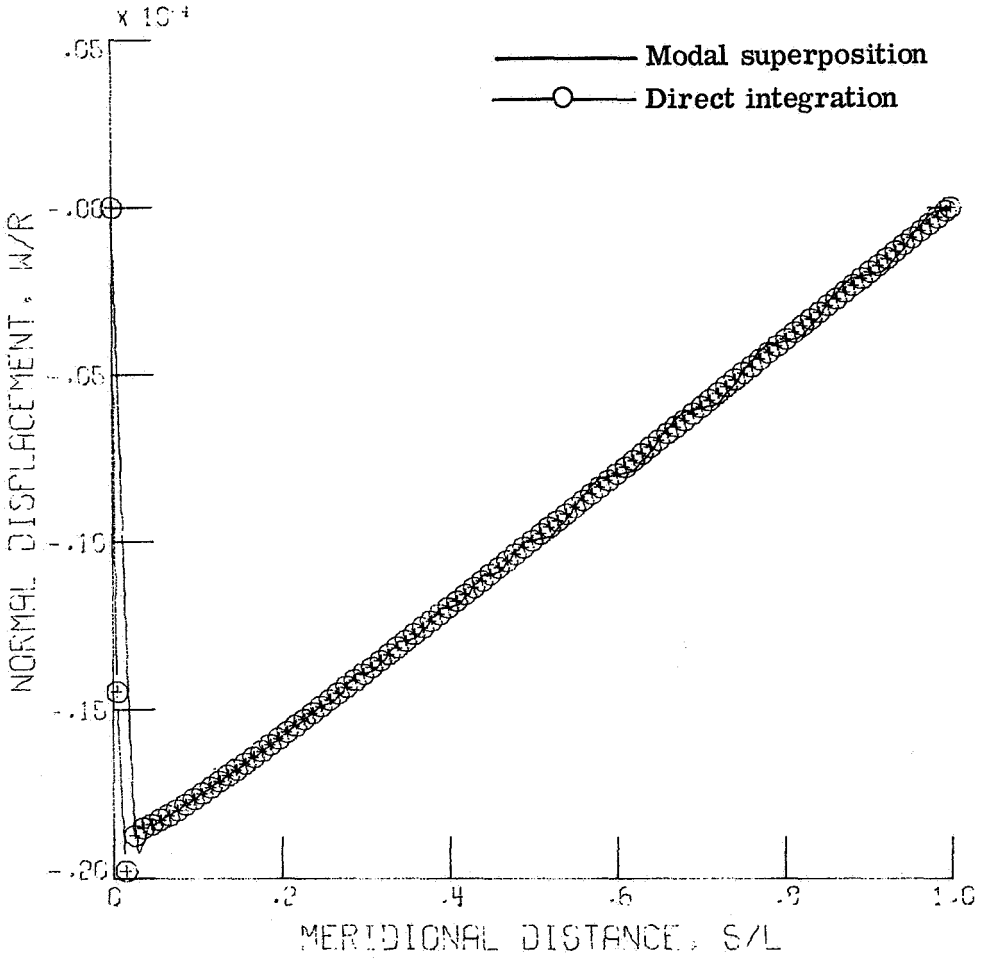

Figure 14.- Comparison of methods for the conical shell at $n = 2$ and $t = 20 \times 10^{-6}$ sec.

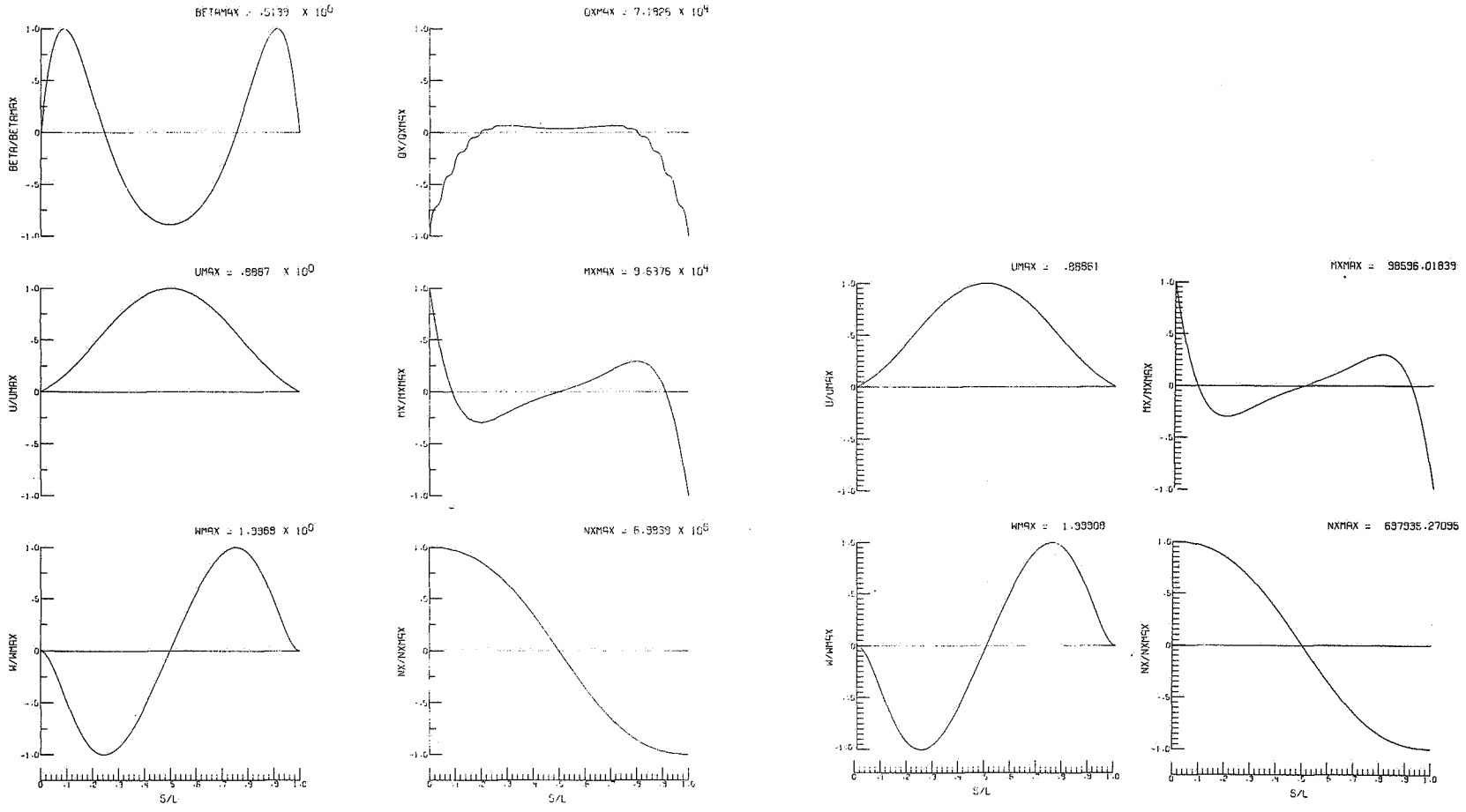

Present analysis

Reference 7

(a) First mode.

Figure 15.- Mode shapes, modal stress resultants, and modal moment resultants for clamped-clamped cylinder.

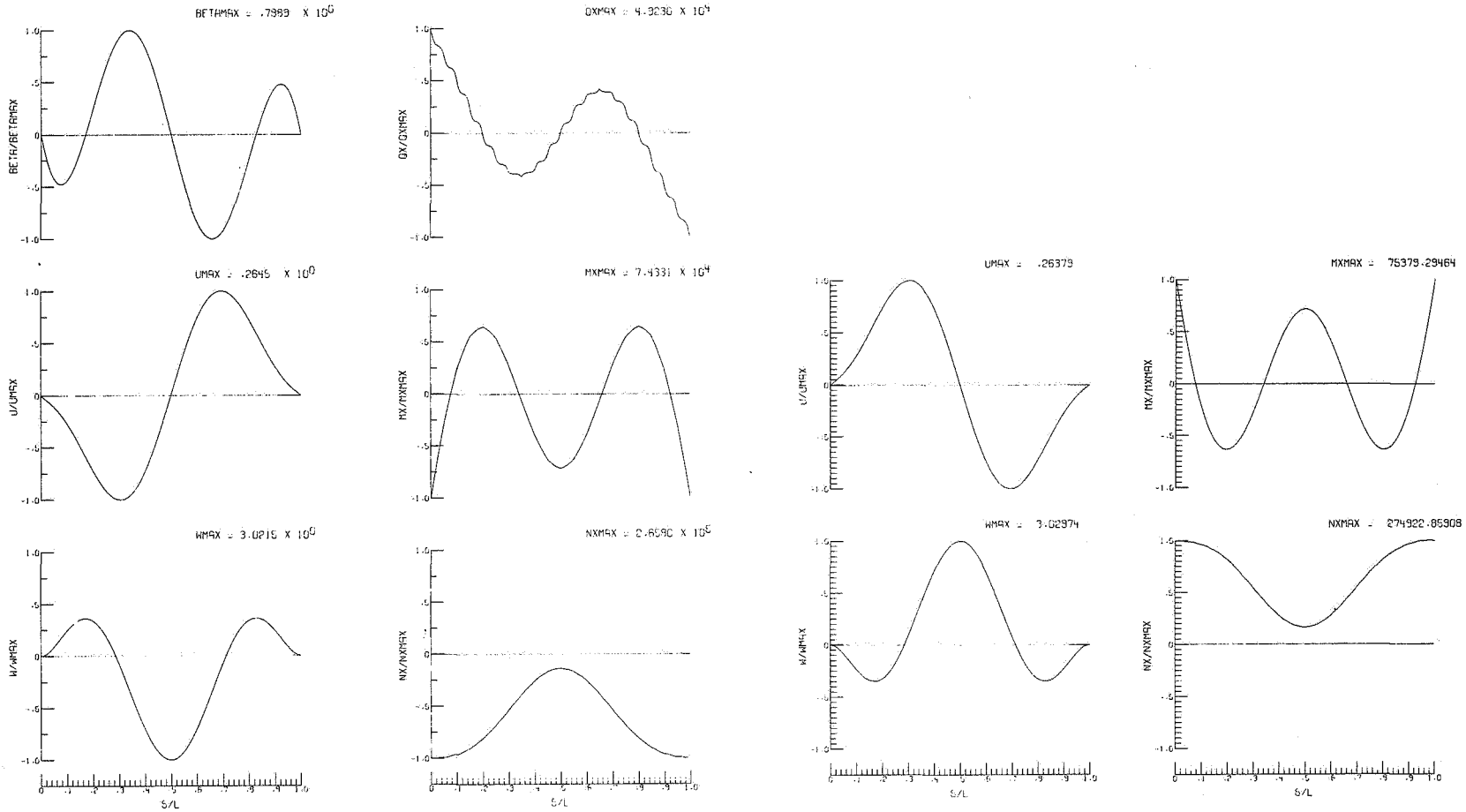

Present analysis

Reference 7

(b) Second mode.

Figure 15.- Continued.

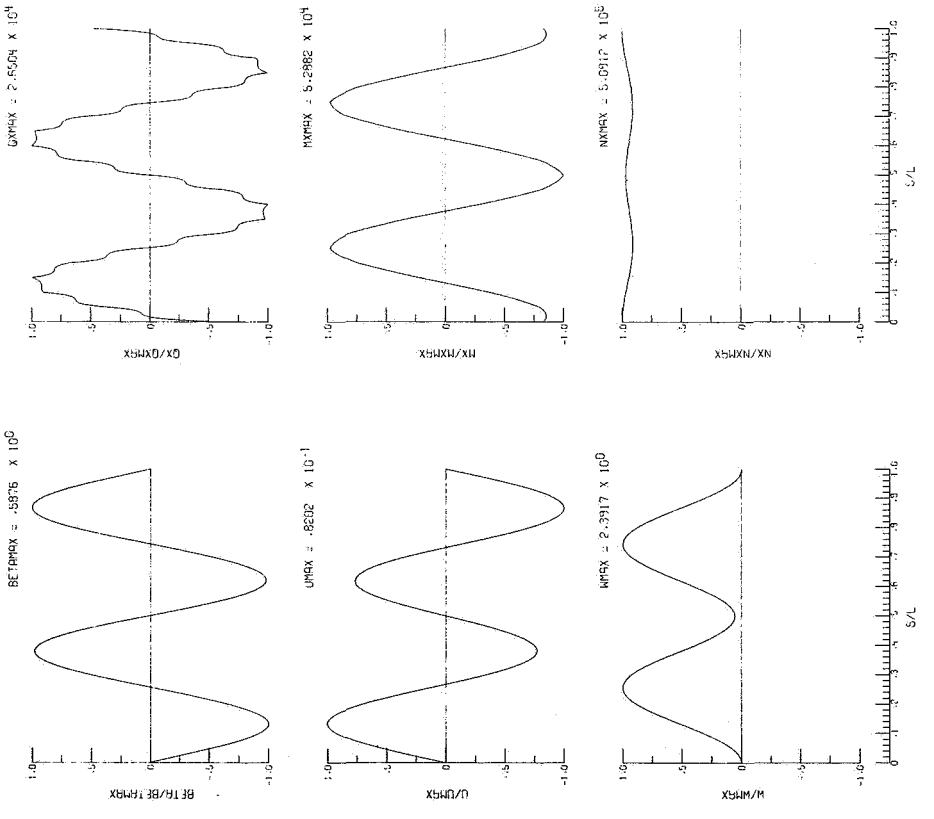

(c) Third mode.

Figure 15.- Continued.

NATIONAL AERONAUTICS AND SPACE ADMINISTRATION
WASHINGTON, D.C. 20546

OFFICIAL BUSINESS
PENALTY FOR PRIVATE USE $300

SPECIAL FOURTH-CLASS RATE
BOOK

POSTAGE AND FEES PAID
NATIONAL AERONAUTICS AND
SPACE ADMINISTRATION
451

U.S. MAIL

POSTMASTER: If Undeliverable (Section 158
Postal Manual) Do Not Return

"The aeronautical and space activities of the United States shall be conducted so as to contribute . . . to the expansion of human knowledge of phenomena in the atmosphere and space. The Administration shall provide for the widest practicable and appropriate dissemination of information concerning its activities and the results thereof."

—NATIONAL AERONAUTICS AND SPACE ACT OF 1958

NASA SCIENTIFIC AND TECHNICAL PUBLICATIONS

TECHNICAL REPORTS: Scientific and technical information considered important, complete, and a lasting contribution to existing knowledge.

TECHNICAL NOTES: Information less broad in scope but nevertheless of importance as a contribution to existing knowledge.

TECHNICAL MEMORANDUMS: Information receiving limited distribution because of preliminary data, security classification, or other reasons. Also includes conference proceedings with either limited or unlimited distribution.

CONTRACTOR REPORTS: Scientific and technical information generated under a NASA contract or grant and considered an important contribution to existing knowledge.

TECHNICAL TRANSLATIONS: Information published in a foreign language considered to merit NASA distribution in English.

SPECIAL PUBLICATIONS: Information derived from or of value to NASA activities. Publications include final reports of major projects, monographs, data compilations, handbooks, sourcebooks, and special bibliographies.

TECHNOLOGY UTILIZATION PUBLICATIONS: Information on technology used by NASA that may be of particular interest in commercial and other non-aerospace applications. Publications include Tech Briefs, Technology Utilization Reports and Technology Surveys.

Details on the availability of these publications may be obtained from:

SCIENTIFIC AND TECHNICAL INFORMATION OFFICE

NATIONAL AERONAUTICS AND SPACE ADMINISTRATION

Washington, D.C. 20546